Three-dimensional ultrasound imaging

R W Prager*, **U Z Ijaz, A H Gee,** and **G M Treece**
Department of Engineering, University of Cambridge, Cambridge, UK

The manuscript was received on 23 January 2009 and was accepted after revision for publication on 8 June 2009.

DOI: 10.1243/09544119JEIM586

Abstract: This review is about the development of three-dimensional (3D) ultrasonic medical imaging, how it works, and where its future lies. It assumes knowledge of two-dimensional (2D) ultrasound, which is covered elsewhere in this issue. The three main ways in which 3D ultrasound may be acquired are described: the mechanically swept 3D probe, the 2D transducer array that can acquire intrinsically 3D data, and the freehand 3D ultrasound. This provides an appreciation of the constraints implicit in each of these approaches together with their strengths and weaknesses. Then some of the techniques that are used for processing the 3D data and the way this can lead to information of clinical value are discussed. A table is provided to show the range of clinical applications reported in the literature. Finally, the discussion relating to the technology and its clinical applications to explain why 3D ultrasound has been relatively slow to be adopted in routine clinics is drawn together and the issues that will govern its development in the future explored.

Keywords: three-dimensional ultrasound, medical imaging, clinical applications

1 INTRODUCTION

Three-dimensional (3D) ultrasound was first demonstrated in the 1970s and in 1989 the first commercial 3D scanner, the Kretz Combison 330, became available. Since then, the quality of 3D scanners has improved and the range of clinical applications has grown. However, 3D facilities are still offered only on high-end scanners and there has not been a rush to replace two-dimensional (2D) scanners with 3D scanners in general clinical practice.

Previous researchers have covered the fundamental technology [**1**, **2**], functionality, and applications [**3**, **4**] of 3D ultrasound. In this review, recent progress is described and attempts are made to set it in the historical context of the developing field. This paper explores whether the real-time 2D ultrasound scanner is fundamentally the best design for medical imaging or whether, in time, 3D ultrasound will supersede 2D ultrasound, as 2D scanning itself superseded one-dimensional (1D) A-line scanning. In order to explore this issue, it is necessary to understand how 3D ultrasound data are acquired, processed, and visualized. It is also necessary to see what clinical applications are likely to benefit from 3D data. Against these benefits, the disadvantages inherent in the various approaches to 3D must then be balanced.

3D ultrasound is most commonly acquired in one of three ways (Fig. 1). The most obvious approach, although the most difficult to achieve, is to have a 2D array of transducer elements in contact with the object to be scanned (Fig. 1(c)). This can record 3D data directly by firing and receiving with different combinations of elements. Because dense arrays of 2D transducers are difficult to build, alternative approaches have been developed using 1D transducer arrays to produce 2D B-scan images at known locations in 3D space. The second group of acquisition strategies involves sweeping the 1D transducer array through a known trajectory using a mechanical device (Figs 1(a) and (b)). The third group of acquisition strategies involves letting the clinician sweep the 1D transducer array manually across the subject and using some sort of tracking device to measure its trajectory (Fig. 1(d)).

**Corresponding author: Department of Engineering, University of Cambridge, Trumpington Street, Cambridge CB2 1PZ, UK.*
email: rwp@eng.cam.ac.uk

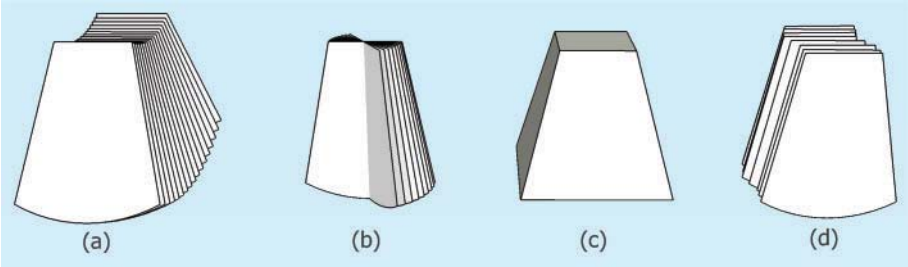

Fig. 1 The form of the data acquired in four different types of 3D ultrasound, where in (a), (b), and (d) each outline symbolizes a B-scan with the probe (not shown) at the top pointing downwards: (a) the structure of the data from a mechanically swept probe; (b) the form of the data when the probe is mechanically rotated about its axis; (c) the outline of a pyramidal volume that might be acquired by a 2D transducer array, where again the probe would be above the diagram, pointing downwards; (d) the clinician moves the probe over the subject and a sensor is used to record its trajectory. In (a), (b), and (d) the B-scan slices would normally be closer together than shown in the diagram

1.1 Where does 3D ultrasound offer a clinical advantage?

At the simplest level, 3D ultrasound contributes to eliminating operator dependence in the scanning process. 2D ultrasound requires the clinician to sweep the probe back and forth across the subject while mentally visualizing the anatomy from multiple 2D images. 3D, on the other hand, often requires only the acquisition of a single volume. Once this has been acquired it can be visualized using slices at any angle and a variety of measurements may be taken from it. Furthermore, 3D data enable 3D visualization techniques such as volume rendering and surface rendering to be employed.

Quantitative estimates in 2D ultrasound are based on heuristic formulae with strong prior assumptions which are prone to error. 3D ultrasound provides a more accurate and repeatable way of evaluating anatomic structures and disease entities [**5**]. This repeatability also makes 3D more suitable than 2D for monitoring the progression of a disease or its response to treatment [**6**–**8**]. The ability to acquire a 3D block of data makes it easier to register the ultrasound with other modalities and, for the case of intra-operative scanning, with scans acquired before the operation [**6**].

3D scanning has been shown to facilitate ultrasound-guided biopsy as arbitrary planes, not available in a conventional 2D scan, can be chosen and visualized in real time [**9**]. For example, 3D endorectal ultrasound has been used for staging and biopsy in rectal cancer [**10**]. 3D ultrasound has been reported as having potential as a safe low-cost alternative to the conventional 2D X-ray-based breast examination [**11**]. It has also been used to scan for fetal [**12**] and gynaecological [**13**, **14**] anomalies.

The remainder of the paper is structured as follows. The three main methods of 3D ultrasound acquisition are discussed in sections 2, 3, and 4. Techniques for processing and visualizing 3D ultrasound are described in section 5. A comprehensive table of clinical applications is presented in section 6 and the paper ends with some speculation about the future development of the field in section 7.

2 ACQUISITION USING A MECHANICALLY SWEPT TRANSDUCER

Currently, the most common type of commercial 3D ultrasound scanner is that based on a mechanically swept probe or 'wobbler'. A 1D transducer array, similar to that in a conventional probe, is mounted inside a housing and moved mechanically through a known trajectory. This enables the acquisition of a regular pattern of 2D scans covering a fixed 3D volume.

Most of the development of these systems took place in an industrial rather than an academic context. Therefore they will be discussed with reference to the work of a company, Kretztechnik AG (Zipf, Austria), who have been a major contributor in this field. The company was founded in 1947 and moved into ultrasonic medical instrumentation in the 1950s. In 1989 they produced the first general-purpose, mechanically swept 3D ultrasound system, the Combison 330. The company was bought by Medison in 1996 and in 2001 it was sold again, this time to General Electric (GE). Kretztechnik is now a wholly owned subsidiary of GE Medical

Systems (see the excellent concise online history of the company by Woo [**15**]).

Figure 2 shows the internal structure of a classic Kretztechnik probe, the RSP6-12, a 3D small-parts probe working from 6 MHz to 12 MHz with 192 transducer elements. A Phytron stepper motor (Phytron Elektronik GmbH, Gröbenzell, Germany) drives a planetary gearbox. The yoke with the array of transducer elements is mounted on the output of the gearbox. In Fig. 2(a) the stepper motor is the black part of the cylinder (mounted across the probe near the connection to the cable) and the gearbox is the metallic part of the cylinder. The yoke can be seen connected to the spindle at the end of the gearbox. It is also mounted on a freely rotating joint at the motor end of the cylinder. The yoke disappears into a black bag, together with a large number of wires. These are the wires to drive the transducer elements. The black bag joins on to the rectangular scanning window that forms the probe face. The space between the bag and the probe face contains the transducer array, mounted on the end of the yoke, and is filled with an oily substance.

Figure 2(b) shows the side of the probe nearest the stepper motor. The miniature circuit board serves two purposes. It connects each of the four stepper motor wires to two of the wires in the main cable and includes circuitry to support the two sensors that detect the position of the transducer yoke. There is one Hall-effect proximity sensor monitoring the motor shaft (visible near the motor axle with three wires coming out of it), and another to monitor the position of the transducer yoke (just below the first sensor). There is thus one sensor before the gearbox and one after it. The motor shaft sensor detects one orientation of the shaft; it is thus activated once every motor revolution. The yoke sensor detects when the yoke is approximately in its central position. The sensors are configured to operate in series; only when they are both aligned is the appropriate signal generated. This happens when the transducer yoke is exactly in the middle of its range of movement: top dead centre. In order to determine the position of the yoke, it is necessary to search using the stepper motor until both sensors line up. Once alignment has been achieved using the sensors, the yoke can be moved to other positions by counting steps with the stepper motor. The stepper motor drive wires are wrapped up in the same probe cable with the 192 wires from the crystal elements. It

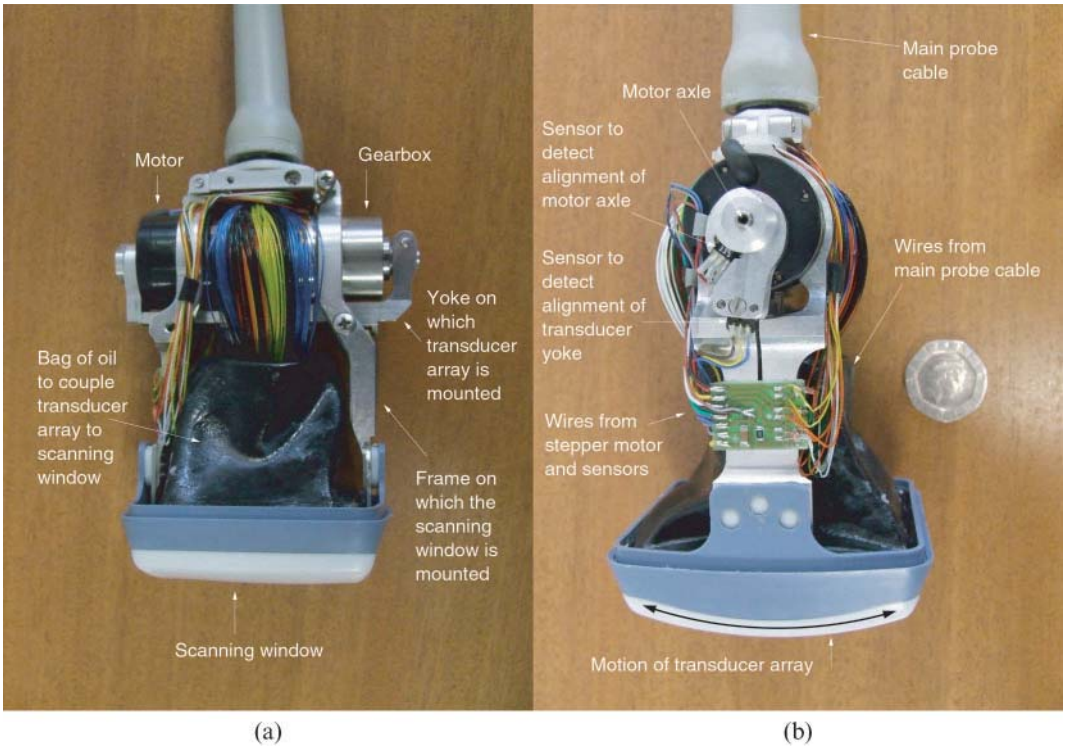

Fig. 2 The Kretztechnik (GE Medical Systems) RSP6-12 probe: (a) the side of the probe showing the transducer wires, gearbox and yoke on which the transducer array is mounted; (b) the end of the probe showing the two sensors and the miniature circuit board. The transducer array sweeps from side to side in image (b). The coin is the UK 20p piece and is included for scale. It is about 21 mm in diameter

is therefore necessary to avoid the generation of high-frequency transient currents by the stepper motor driving circuitry which could create noise in the ultrasound radiofrequency (RF) data.

The mechanical design, even at this coarse level, is remarkably elegant. Equally clever is the way that ultrasound is smoothly coupled from the transducer array across the oil and scanning window into the subject. There are few artefacts and, despite the complexity of the beam path, the probe is able to focus effectively both elevationally and laterally.

The 1D transducer array, mounted on the yoke, is superficially similar in design to a conventional probe. It is focused elevationally using an acoustic lens and in the lateral direction by controlling the delays associated with each of the crystals which are fired to generate a particular A-line of RF data. When the yoke is stationary, it produces B-scans in the normal way. It is possible to drive such a transducer in a quasi-static mode. The stepper motor is driven to position the yoke, next a B-scan is acquired, and then the stepper motor moves again, followed by another acquisition. In this case, the yoke is stationary while each B-scan is recorded. This is simple to understand and implement, but too slow for most clinical requirements. In practice, the yoke starts from one side, accelerates, moves smoothly across the scanning window, and then decelerates at the other side. The ultrasound machine acquires data continuously at a high frame rate during this process. The location of each acquired B-scan can be computed by coordinating the instructions given to the stepper motor with the timing of the ultrasound excitation. The fact that the transducer is moving during the acquisition process affects the data. At a simple level, the B-scans will be stretched and twisted slightly, relative to equivalent B-scans from quasi-static acquisition. This is because the yoke will change position between the time when the first and the last A-line of a particular B-scan are acquired. The faster each B-scan can be acquired, the faster the yoke can be driven while maintaining satisfactorily dense sampling of the 3D scan volume. More sophisticated approaches to beam forming have therefore been developed. For example, more than one A-line can be acquired simultaneously at different points along the transducer surface.

Other groups and companies have also contributed significantly to the development of mechanical 3D probes and techniques for processing their data. All the major manufacturers now offer some sort of 3D facility. Particular work on miniature 3D devices for urological and surgical applications was done by BK Medical (Herlev, Denmark), established in 1976 as a division of Brüel & Kjær but now owned by Analogic Inc. TomTec (Unterschleissheim, Germany), were for many years leaders in the design of mechanical systems in which the probe is twisted about its centre-line. This results in the acquisition of a set of radial slices all centred on the same axis (see Fig. 1(b)). They now specialize in working with other equipment manufacturers in the fields of 3D and time-varying 3D ultrasound.

When data are acquired using a mechanically swept probe, the acquisition volume and the relative location of each A-line inside it are known in advance. It is therefore possible to have a plan for rasterizing the data as it is acquired and to perform this task using efficient digital signal-processing hardware. A compromise between the sparse sampling at the periphery of the sweep and the denser sampling close to the probe is struck in advance, and the scanner produces a real-time volume in a similar way to how a 2D scanner with a curvilinear probe produces a real-time rasterized B-scan [**16**].

Mechanically swept 3D probes are currently used in all but the fastest applications (such as echocardiography [**17**]), since their resolution is generally better than that currently available from 3D probes based on 2D transducer arrays (see section 3). This is because 3D probes based on 2D transducer arrays are new technology and mechanical probes are very mature. In time, it is expected that 2D transducer arrays will continue to develop and eventually will eclipse the mechanical devices in terms of both performance and production cost [**18**].

If a fetus is surrounded by a reasonable amount of amniotic fluid, then its 3D skin surface can be computed using an algorithm based on smoothing and gradient operators. This means that it is possible automatically to surface render the fetal face in 3D which is a very attractive facility for parents. Figure 3 shows some nice examples. Sometimes, images of this sort are produced as a by-product of clinical scans; sometimes, extra scanning is performed to generate the images because clinicians believe that they enhance the growing bond between the mother and fetus in a beneficial way; sometimes, the parents just pay to have the extra scans (although professional societies are generally opposed to scanning without appropriate medical justification).

3 ACQUISITION USING A 2D TRANSDUCER ARRAY

A conventional probe for acquiring 2D B-scans typically has at least 128 transducer elements along

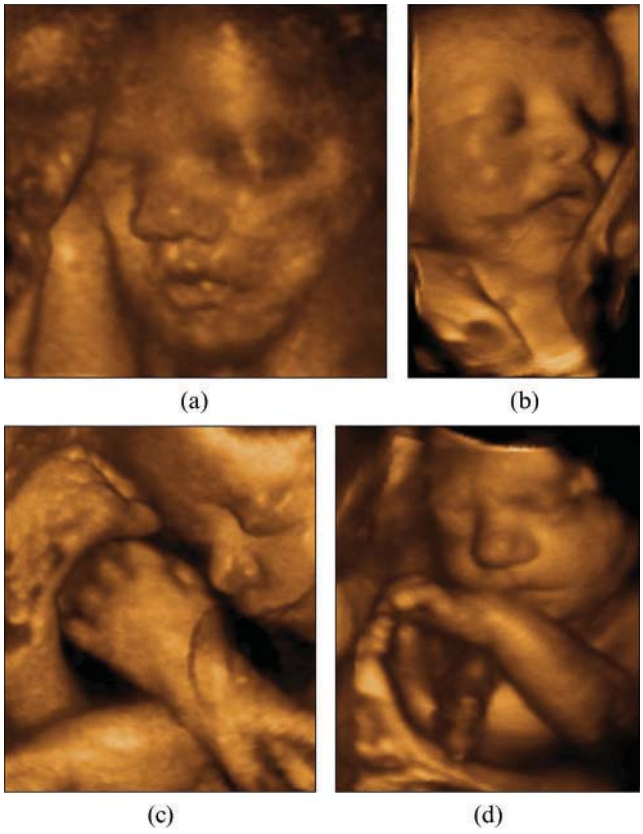

Fig. 3 Images of fetal faces *in utero* derived from 3D and four-dimensional scans using a GE Voluson 730 Expert machine with a 3D mechanically swept probe. (Images courtesy of Martha Morgan, Little Sprout Imaging, Towson, Maryland, USA)

its length. This suggests that ideally a 2D transducer array would have $128 \times 128 = 16\,384$ elements arranged in a rectangular grid. This requirement poses several problems.

It is possible to make such a transducer array with current technology; this is not the main difficulty. The apparently simple problem of connecting wires to each of the elements without distorting the mechanical structure of the transducer assembly is a formidable challenge [**19**].

Another major challenge relates to speed. 2D scanners typically generate up to 100 B-scans a second using a simple sweeping pattern with a single lateral transmit focus. Considered from another viewpoint, 128 sound beams travelling 10 cm out and 10 cm back takes about $\frac{1}{60}$ s at 1540 m/s. This means that 16 384 beams would take 2.1 s, which is far too slow. Therefore a parallel beam former is required to enable multiple receive foci for each transmit pattern. This implies that it is necessary to process the data from quite a large proportion of the transducer elements in parallel. (A hypothetical design with 128 transducer elements and 128 A-lines (sound beams) has been described. The number of transducers does not necessarily have to correspond to the number of A-lines. The creation of each A-line requires an active aperture formed of many transducer elements and this can be positioned arbitrarily across the face of the probe.)

This brings us back to the topic of wiring. If all 16 384 elements were connected up with a suitable individual wire, it would result in a cable about 68 mm in diameter. Clearly, some sort of signal multiplexing is vital, but this needs to be carried out in a way that does not prevent the parallel beam forming that is required for speed. Both these problems are solved if the analogue-to-digital conversion and beam-former control can be miniaturized and mounted in close proximity to the transducer array, in the probe body itself.

Having obtained an idea of the challenges involved, the way in which the field has developed is now looked at. In the early 1990s, Smith *et al.* [**20**] at Duke University built a 2D piezoelectric transducer array with 20×20 elements of which 32 could transmit and 32 could receive at any one time. Phased-array beam forming was used to scan a pyramidal volume. By 2004 the same group produced a variety of arrays from 40×40 to 80×80 with up to 440 transmit and 256 receive channels [**21**, **22**]. They also constructed a rectilinear scanner with a 128×128 grid of transducer elements to image a rectangular volume using 169 large transmit blocks and up to 1024 multiplexed receive elements [**23**, **24**].

At the University of Oslo, Austeng and Holm [**25**] have also worked on sparse arrays of piezoelectric transducers. They used a grid of 48×48 elements of which up to 32 can be active in receive and transmit at any one time. The amplitude of the ultrasound beam side lobes can be reduced either by using an irregular arrangement of active elements or by curving the transducer array in one dimension [**26**].

Commercial 2D piezoelectric arrays are now being produced in parallel with academic research [**18**]. For example, Philips is currently offering a range of phased-array probes, running at between 1 MHz and 7 MHz, with up to 2880 fully connected elements. This employs a transducer grid slightly larger than 50×50 and a pyramidal acquisition volume.

Tiny piezoelectric transducers in a 2D grid have a higher impedance than the larger transducers found in the 1D arrays that produce B-scans. There is therefore more likely to be a mismatch between the

crystal impedance and the characteristic impedance of the connecting cable. This difficulty does not arise in capacitative micromachined ultrasonic transducers (CMUTs). These devices consist of parallel-plate capacitors, about 30 μm across, fabricated on the surface of a chip, such that one plate is caused to vibrate by a varying voltage (Fig. 4). They have better bandwidth than piezoelectric devices [**27**], and the transducer chip can be directly bonded to another chip carrying driver circuitry using the 'flip-chip' technique. This removes the need to attach individual 'wires' to the elements altogether. One difficulty is that a high voltage would be required to produce sufficient acoustic amplitude from an individual transducer element on its own and it is not practical to generate these voltages on the closely bonded chip. This problem can be overcome by forming each element of the array from a number of smaller capacitors working in parallel. These smaller devices can be driven with lower voltages that can be controlled effectively on the locally bonded driver chip.

A group at Stanford has been active in this area for some time and has produced a 16×16 array, flip-chip bonded to a custom driver integrated circuit [**28**–**30**]. Simulation studies of this sort of device have been conducted in Rome [**31**]. Sensant Corporation was involved in developing CMUT ultrasound transducers in an industrial context and in June 2005 they were taken over by Siemens. The University of Madison, Wisconsin have been working with Siemens to exploit the improved bandwidth of their prototype CMUT-based 3D probe for tissue characterization [**27**, **32**].

Rather than building a miniature assembly of transducer elements to record a 3D scan, an alternative approach is to mount a large number of transducers in a fixed configuration around the subject. An example of this is illustrated for breast scanning in Fig. 5. Insonification and data acquisition from many different directions give enhanced 3D resolution. They also enable the estimation of attenuation, sound speed, and backscatter. However, in some versions of such a system the scanning and

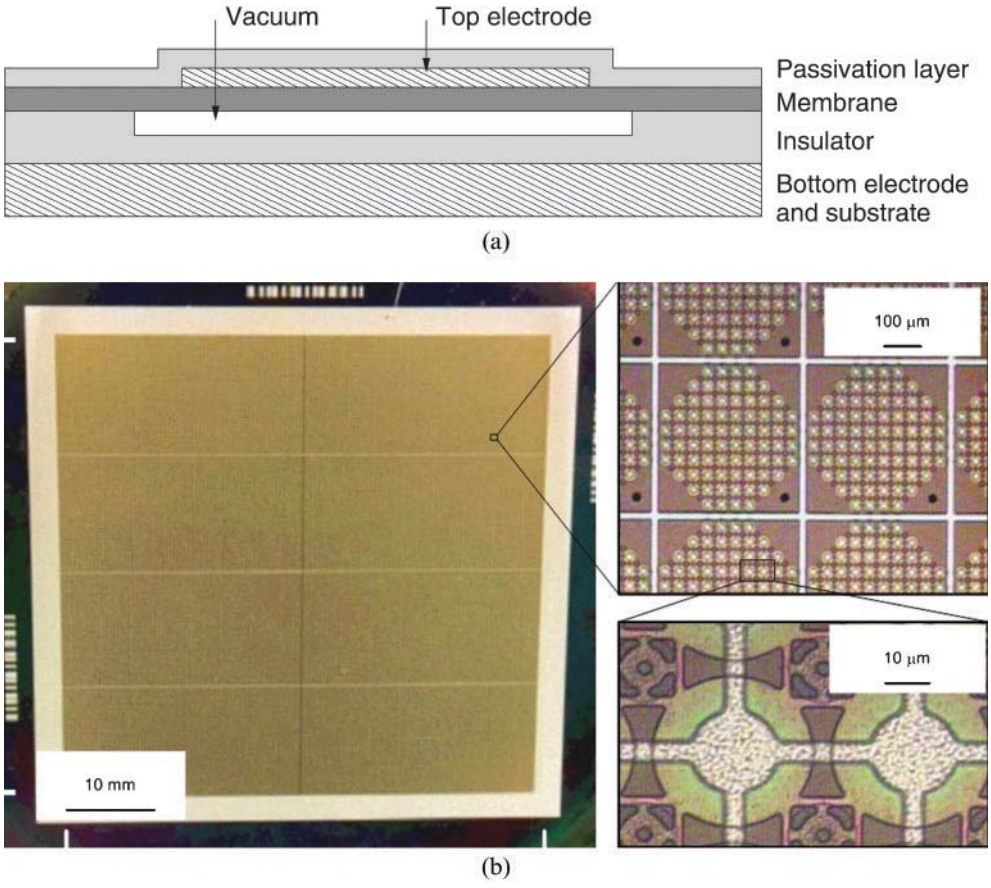

Fig. 4 Structure of CMUTs: (a) schematic diagram of a single transducer element; (b) a 2D array of transducer elements. (Figures courtesy of Professor B. (Pierre) T. Khuri-Yakub, Stanford University)

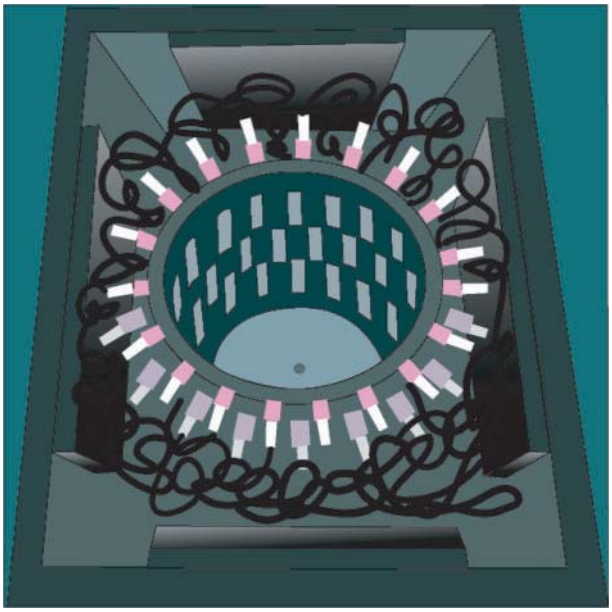

Fig. 5 A 3D ultrasound system consisting of a cylinder with transducers arranged around the periphery. There are 48 transducer arrays with 32 receivers and eight emitters in each array. The assembly can be rotated into six positions to enable transmission and reception from even more locations. Emitters are activated individually and both the reflected and the transmitted signals are recorded by many receivers. This enables the estimation of the speed of sound and attenuation as well as backscatter. The acquisition and reconstruction processes are currently too slow for clinical applications. It is hoped that a system such as this will eventually be used for early breast cancer detection and diagnosis [**11**]

data-processing procedures are currently too slow, and in all implementations it is only possible to scan things that fit inside the cylinder of transducers [**11**]. Other systems that employ a similar approach include the Techniscan product [**33**], with two opposed transducer arrays that rotate around the breast and the CURE system developed at the Karmanos Cancer Institute [**34**–**36**].

4 FREEHAND ACQUISITION

3D ultrasound data can be acquired using a six-degrees-of-freedom position sensor and a 1D transducer array that produces a sequence of 2D B-scans. This is called *freehand 3D ultrasound* [**37**]. (Some workers use the term 'tracked ultrasound' when an external position sensor is used and the term 'freehand 3D ultrasound' when there is no external sensor. Here both the tracked and the untracked systems are referred to as freehand 3D ultrasound.) The position sensor is fixed rigidly to the ultrasound probe. As the clinician scans the region of interest, its trajectory and orientation are recorded, together with the sequence of acquired 2D B-scans. This information subsequently enables each 2D B-scan to be located in 3D space, forming an inhomogeneous 3D data block.

A freehand 3D ultrasound system consists of a conventional ultrasound machine, a position sensor, and a computer to record the B-scans and positions (Fig. 6). Most commonly, a magnetic or optical position sensor has been used [**38**, **39**].

In a magnetic position sensor a time-varying 3D magnetic field is transmitted throughout the volume in which the scan is to be acquired. Three small coils are attached to the probe and used to pick up the field in three orthogonal directions (Fig. 7). This information enables the position and orientation of the coils to be computed. Published work has centred around the Bird sensors from Ascension Technology Corporation (Burlington, Vermont, USA) [**40**], the Fastrak sensor from Polhemus (Colchester, Vermont, USA) [**41**], and the Aurora from Northern Digital (Waterloo, Ontario, Canada) [**42**]. The Fastrak and Aurora use an alternating magnetic field whereas the Bird uses a pulsed field.

The main attraction of using a magnetic sensor is that there does not need to be a clear line of sight between the transmitter and the receiver. The main disadvantage is the need to keep metal, particularly ferromagnetic metal, out of the area. Hastenteufel *et al.* [**43**] suggested that sensors based on alternating fields are generally more sensitive to metal because of their vulnerability to eddy currents, whereas pulsed systems are particularly sensitive to ferromagnetic materials. The metal beds used in hospitals can be particularly inconvenient. Special magnetic transmitters have been developed to fit between the patient and the bed in an effort to overcome this difficulty [**44**].

When an optical tracking system is used, either a passive or active target is attached to the probe and this target is tracked by two (or more) calibrated cameras (see Fig. 6). A passive target might consist of an arrangement of three or more matt spheres at known relative positions on a small frame. An asymmetry in the arrangement of the spheres can enable the tracker to infer the orientation of the frame. An active target may be formed from an arrangement of infrared light-emitting diodes (LEDs) that are excited in a known sequence, synchronized

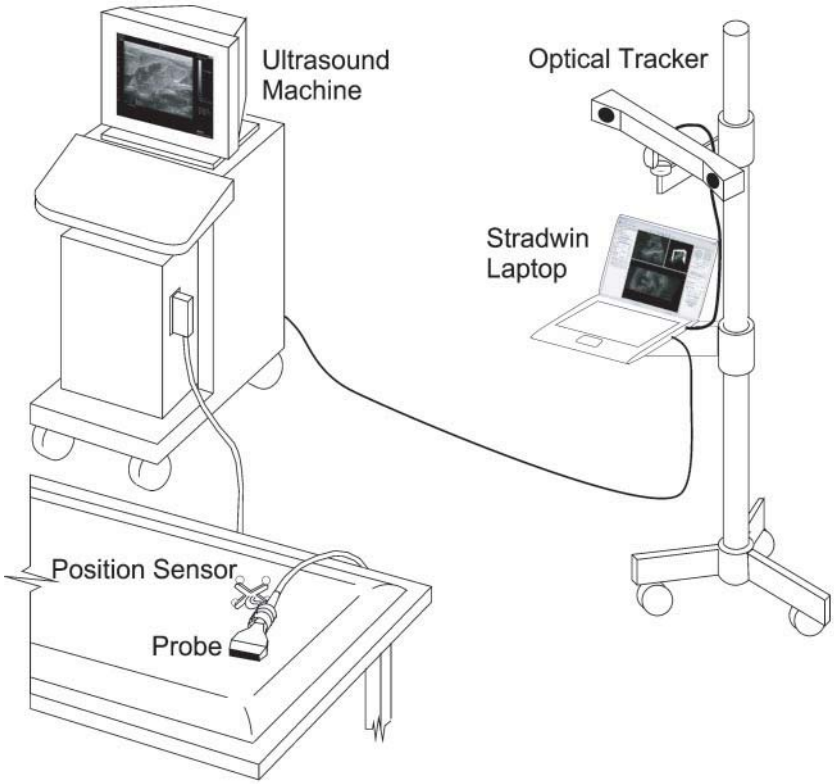

Fig. 6 General arrangement of a freehand 3D ultrasound system using an optical position sensor. The three spheres attached to the probe are tracked by calibrated cameras. The laptop records the 2D ultrasound images together with the position and orientation of the probe at the point at which each image was acquired

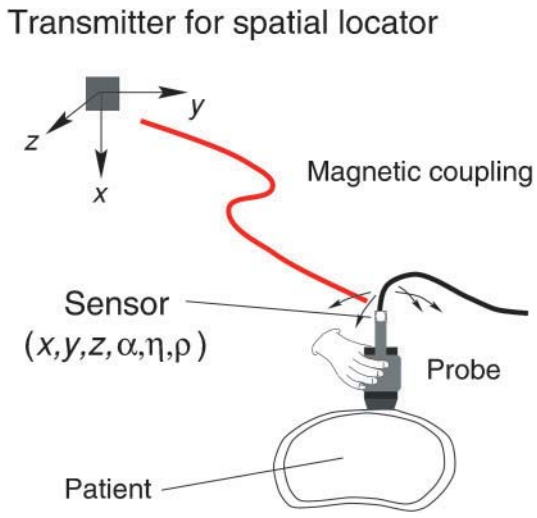

Fig. 7 The transmitter generates time-varying magnetic fields at different orientations. A sensor is attached to the probe which picks up the fields in three orthogonal directions and computes its location (three translations x, y, and z), and orientation (three Euler angles α, η, and ρ), from this information

with the tracking software used with the cameras. This enables the system to identify individual LEDs and hence to infer the orientation of the complete assembly.

There are a number of commercial optical tracking systems available that can be used to acquire freehand 3D ultrasound. The Polaris system from Northern Digital has been used by several groups including our own [**45**, **46**]. Optical trackers are particularly good at locating absolute positions and orientations in 3D space relative to the calibrated cameras. They can provide an indication of whether each position reading meets a specified accuracy whereas it is sometimes difficult to tell how much magnetic systems have been affected by metal in the environment [**47**, **48**]. However, they have the major drawback of requiring the clinician to maintain an uninterrupted line of sight between the cameras and the tracked objects attached to the probe (see Fig. 6). This constraint can be made less onerous by installing a larger number of cameras around the room and only requiring the probe to be visible to a subset of them to produce a reliable reading. This makes the system more expensive and less portable.

Other work has focused on using less obtrusive position sensors that do not provide all six degrees of freedom which are required to locate the position and orientation of the probe. Inertial sensors give the orientation satisfactorily but drift so that the scan must be completed in a limited amount of time. This leaves the translational motion to be determined by another means. A miniature camera can be attached at each end of the probe, facing towards the scanned subject. Motion of the subject surface (typically skin) in the camera images can be combined with orientation information to infer the overall probe translation [**49**, **50**]. Alternatively, the translation may be deduced from the rate at which the probe motion perpendicular to the scan plane causes the speckle pattern in the ultrasound images to decorrelate [**51**].

Even the best position sensors do not provide the location and orientation of the B-scan directly. In addition, the rigid body transformation from the part of the position sensor attached to the probe to the B-scan must be known. The process of determining this is called *spatial calibration*. It is usually accomplished using a phantom-based technique. A specially designed object (the phantom) is scanned in a predetermined way. The phantom is designed so that the acquired data will only be consistent when interpreted using the correct calibration transformation. This allows the calibration to be calculated by some form of optimization or closed-form solution process. The calibration transformation will remain valid as long as the rigid mounting of the position sensor on the probe is not changed. A comprehensive review of 3D ultrasound calibration techniques can be found in reference [**52**].

Neither the ultrasound data nor the position information are delivered to the computer instantaneously. Delays may be introduced by the ultrasound machine, the position sensor, and any communication mechanisms that are used to get all these data into the computer running the 3D ultrasound software. (With appropriate cooperation from the manufacturer, the computer at the heart of the ultrasound machine may also be used to record the freehand 3D data.) If the delays associated with the images and positions are different, then it will be inappropriate to link images and positions that appear to arrive simultaneously. This problem can be solved by time stamping each image and position as early in the acquisition process as possible and assuming that for a particular hardware and software configuration there is a constant delay up to this point. A process of *temporal calibration* is then required to work out the overall delay between corresponding images and positions. This is performed by scanning a phantom in a way that produces a predicatable time-varying response in the ultrasound image. For example, a flat surface can be scanned with a steady motion in which the distance between the surface and the probe increases and decreases. This results in a line that moves up and down the ultrasound image. The temporal calibration may then be estimated by aligning the motion of the line with the motion recorded by the position sensor [**53**, **54**].

Hitherto the discussion has focused on recording *B-scan images* together with corresponding position and orientation information. It is indeed possible simply to record the B scans as they appear on the screen of the 2D ultrasound machine. The majority of the work in freehand 3D ultrasound has been performed in this way. However, it is also possible to record the RF data from the ultrasound machine, after the receive beam forming and time-gain compensation but before envelope detection or logarithmic compression. This provides data with a greater dynamic range that includes the phase of the ultrasound signal. It can be used to perform freehand 3D strain imaging [**55**], or to improve the resolution perpendicular to the B-scans using data from neighbouring slices [**56**].

Once the freehand acquisition process is complete, a sequence of 2D image slices that can be located in 3D space is obtained. There are now two alternative ways to proceed. The data can be either resampled on to a regular grid [**57**, **58**], or visualized and measured directly from the raw inhomogeneous data.

A major advantage for the resampling approach is its simplicity, but there are also problems. The extra resampling is expensive in both time and computer memory and can lead to a degradation in the quality of the images or the texture of the speckle. The resampling is called *reconstruction*, and the delay that it introduces can be inconvenient in a clinical context. Clinicians often wish to check the quality of a recording immediately after performing the scan but they cannot visualize the data in order to do this until they have gone through the reconstruction process.

The alternative approach to volume measurement and visualization removes the need for the reconstruction operation by using algorithms that work efficiently on the original inhomogeneous data formed of individual slices in 3D space. This was at the heart of the *sequential* approach to freehand 3D

ultrasound that dominated the work in the present authors' group around the turn of the century [**59**] (Fig. 8). The Stradx and Stradwin systems [**60**] perform no unnecessary resampling and enable reslice visualization immediately after a scan has been acquired. (In fact, Stradx is able to do the reslicing live during a scan, if the plane that it is necessary to see is known in advance.)

Tracked ultrasound is used in commercial products where it is important to be able to locate the data in a fixed external coordinate system. Best Nomos (Pittsburgh, Pennsylvania, USA) offer a product called the BAT CAM for ultrasound-guided intensity-modulated radiotherapy. It supports a small-parts probe and a biplanar rectal probe. Resonant Medical (Montreal, Quebec, Canada) offer their Clarity System for image-guided radiotherapy with particular application to the breast and prostate. BrainLAB (Feldkirchen, Germany) integrate tracked ultrasound into their neurosurgery system.

Freehand 3D ultrasound without external tracking is provided by several major ultrasound machine manufacturers as a feature on their higher-end machines. Some use image-based algorithms to control the relative positioning of the B scan slices and hence claim that the resulting data can be used to derive quantitative measurements; others simply provide the facility as a way of producing useful visualizations.

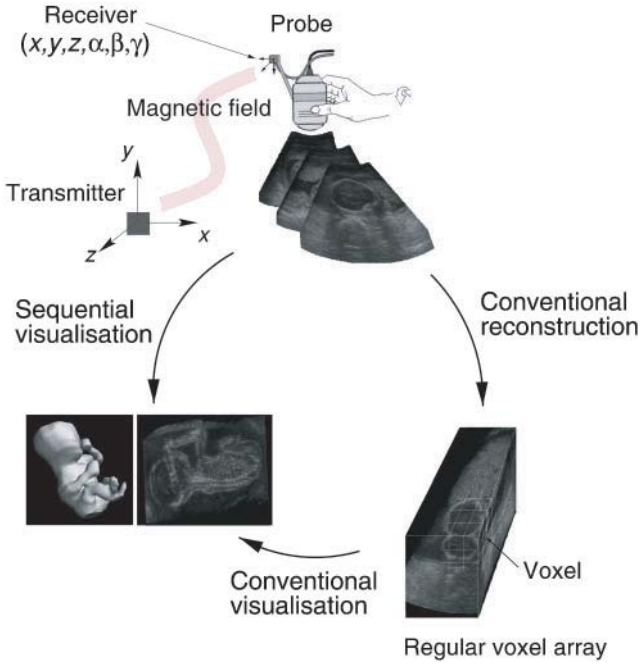

Fig. 8 Two approaches to the initial processing of freehand 3D ultrasound data that have been acquired using a magnetic position sensor. The conventional approach (on the right) involves resampling on to a regular voxel grid before calculating the reslice or volume measurements that are required. The sequential approach makes all calculations in a single step from the acquired inhomogeneous data

Freehand 3D ultrasound has the advantage that it can be performed with a conventional 2D ultrasound machine and so can easily make use of specialist (e.g. high-frequency) probes. When an optical system (or mechanical arm) is used as the tracker, it is possible to locate the acquired data accurately in 3D space. This means that it can be used for radiotherapy or surgery planning [**61**, **62**]. Furthermore, it is possible to acquire 3D data sets of effectively arbitrary dimensions. This can be useful when performing a detailed examination of long structures such as nerves or muscles [**63**].

The disadvantages are the time taken for the 3D acquisition, the need for an external tracking device, and the possibility that the probe pressure may vary during the scan, leading to distortions in the data. In order to ensure that the data are sampled sufficiently densely the clinician has to learn to scan with a smooth trajectory at an appropriate speed. A comparison of the various acquisition strategies that have been discussed is provided in Table 1.

5 PROCESSING AND VISUALIZATION OF 3D DATA

5.1 3D visualization techniques

A common way of handling 3D ultrasound data is to calculate and display the image of a plane through the data. A single image is often called a 'reslice'; alternatively, when more than one resliced-image is involved, it is referred to as 'multi-planar reformatting'. Three orthogonal slice planes are often presented, together with a texture-mapped 3D rendering, showing their relative positions in 3D space. Figure 9 shows this arrangement and Fig. 10 shows a similar tool used with freehand 3D ultrasound. A variety of interpolation algorithms have been used to map from the sampling of the original data to the pixel positions in the reslice. The ubiquitous presence of speckle masks most of the benefit from using the more complex algorithms. Entirely satisfactory and very efficient results can be achieved using nearest-neighbour interpolation [**2**]. Reslice images look superficially like B-scans, but they are not really the same. Most importantly, many of the classic ultrasound artefacts will appear in an unusual form that can be confusing if the direction

Table 1 Comparison of 3D ultrasound acquisition strategies

	Mechanically swept probe	2D transducer array	Freehand + external tracker	Freehand without tracker	Fixed ring of transducers
Scanning system easily moved around	√	√		√	
Fast enough to scan moving structures	√	√			
Can scan arbitrarily large structures			√	√	
Data sampling controlled by machine design rather than scanning motion	√	√			√
Image data located in fixed external coordinates			√		√
More accurate volume and length measurements	√	√	√		√

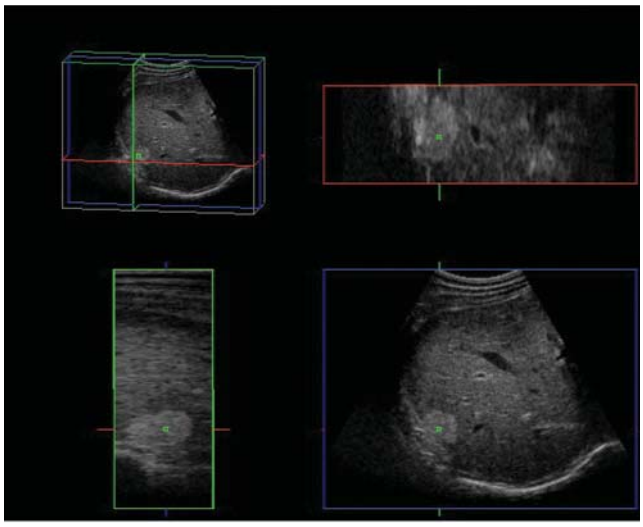

Fig. 9 Orthogonal reslice facility used to visualize a mass in the liver. The orientation of the three reslice images is illustrated by the diagram in the top left corner of the figure. The reslice image in the top right corner of the figure is taken horizontally about one third of the way up the block of data. The reslice image in the bottom right corner of the figure is in the plane of the diagram (top left), about half-way back through the block of data. The reslice image in the bottom left image corner of the figure is taken vertically, perpendicular to the plane of the diagram (top left). The figure was produced using the 3D facilities on the LOGIQ-9 ultrasound system and reproduced courtesy of GE Healthcare

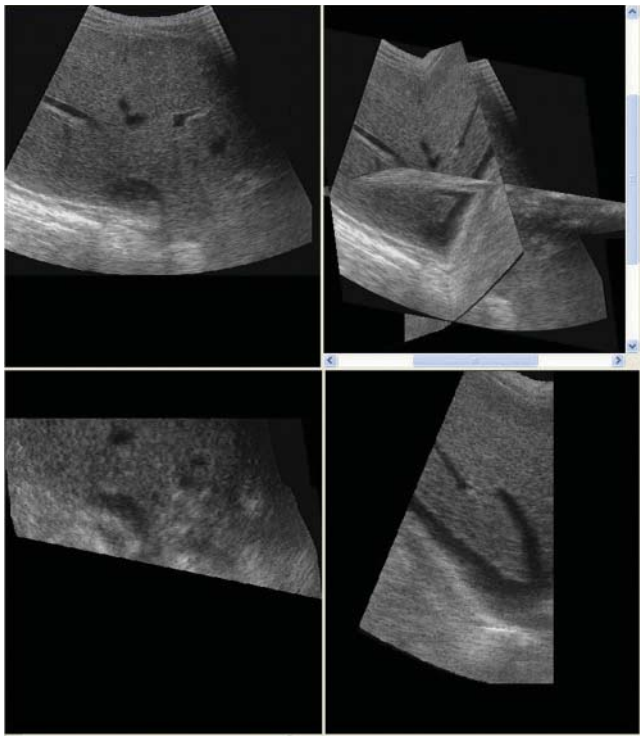

Fig. 10 One original B scan (top left) and two orthogonal reslices (bottom row) through a freehand 3D ultrasound data set of a human liver. The image in the top right corner shows the relative positions of the slices in 3D space

of insonification is not clear. Regions of shadowing or enhancement are hard to spot if the material with particularly high or low attenuation is not in the image. Multiple reflections or reverberations look like genuine data if only part of the repeating pattern is visible [**64**, **65**]. The image resolution and the granularity of the speckle pattern will vary with the angle of the slice. This is because the ultrasound data have different resolutions in the axial, lateral and elevational directions. Nevertheless, if used with care, a reslice tool provides a quick and versatile way to review 3D data and efficiently to visualize complex geometry.

An easy way to obtain a qualitative impression of the salient features of a 3D data block is to volume render it from a sequence of directions and to visualize it from multiple orientations. Volume rendering may be performed directly on the acquired data without prior segmentation. It involves

casting 'rays' through the data, perpendicular to each pixel on the required image. These rays intersect with the voxels of the 3D data (Fig. 11). Each voxel is given properties of brightness, transparency, and sometimes even colour. The value of each pixel in the volume-rendered image is determined by the properties of the voxels that its associated ray intersects [**66**]. A simpler form of volume rendering uses maximum intensity or minimum intensity projection which can both show useful information in appropriate circumstances. These renderings are time consuming to compute, particularly if the underlying data are not sampled on a regular grid (Fig. 12). Nevertheless, special hardware and efficient algorithms have been developed that provide real-time performance for use in a clinical context [**67**, **68**].

5.2 Volume measurement

Volume measurement is a key application in which 3D ultrasound offers advantages over 2D ultrasound. Using 2D ultrasound, a number of measurements are taken and they are used together with a strong prior model to produce a volume estimate. For example, the weight of a fetus *in utero* is often calculated by measuring the biparietal diameter, the abdominal circumference, and the femur length. These numbers are put into a formula that makes some assumptions about the shape and density of an average fetus and produces a weight. Such techniques are accurate in normal healthy cases but the assumptions on which they are based are less reliable in pathological cases, which are by their very nature further from the norm. It is not possible to avoid making assumptions about the density, but with 3D ultrasound the actual volumes can be measured directly, whether or not the shape conforms to an expected norm.

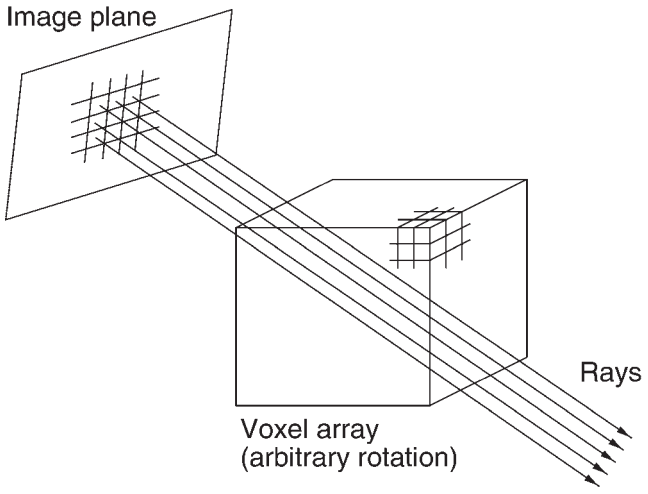

Fig. 11 Volume rendering involving casting rays through the data perpendicular to the required image plane. It is easier to perform if the data are a regularly sampled voxel array

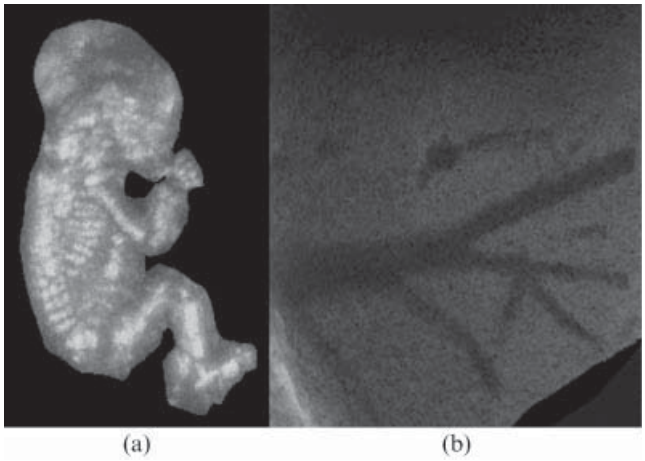

Fig. 12 Volume renderings of slabs of freehand 3D ultrasound: (a) maximum intensity projection of a fetus *in utero* (note that the tissue around the fetus has been excluded from the rendering); (b) minimum intensity projection of a slab 20 mm thick through the liver, showing the blood vessels

The accuracy with which volumes can be measured is dependent on the resolution with which the boundary of the object is imaged. It is generally found that a rotational scanning pattern, as shown in Fig. 1(b), is better than a roughly parallel sweep such as that in Fig. 1(a) [**69**–**71**]. This is probably because 1D transducer arrays have higher resolution in the lateral direction (across the face of the transducer) than in the elevational direction (perpendicular to the B-scan). In a rotational scan, most B-scans will be perpendicular to the object boundary and will therefore measure its location with the (good) lateral resolution. In a parallel scan, the B-scans at the start and end of the sweep will intersect the object boundary obliquely and will therefore only measure its location with the (lower) elevational resolution.

In order to calculate a volume, 3D space has to be divided into two regions: the object and the surroundings. This is the process of segmentation. It can be accomplished manually by providing the clinician with a set of slices through the volume of interest and a tool with which they can 'draw round' the structure to be measured. If the slices are sufficiently close together, efficient algorithms exist to calculate a 3D surface from the set of contours [**72**].

There is a huge literature on automatic and semi-automatic segmentation of medical images. The more automated approaches are useful for X-ray computed tomography and magnetic resonance imaging but work less well for ultrasound. To some extent, this is because of speckle but the other artefacts that characterize ultrasound also contribute significantly to the problem. These include shadowing, enhancement, multiple reflections, and the directional nature of scattering from smooth surfaces such as muscles, vessel walls, and the bladder. In order to be really useful, an automatic or semi-automatic segmentation system must reduce the total elapsed time that the clinician has to spend on the work. A quick algorithm that leaves a small number of errors is of limited value if it takes a long time to find and correct the errors. Even if the algorithm often produces a completely correct segmentation, it is still necessary to take into account the time that the clinician has to spend checking the result before they have confidence in it.

Nevertheless, automatic and semi-automatic techniques can be useful in specific applications [**73**–**77**]. Domain-specific information can be incorporated into the algorithms, resulting in improved segmentation times and reduced intra- and inter-operator variability [**73**, **78**, **79**]. Once a representation of a segmentation is available in three dimensions, standard techniques from computer graphics and computational geometry may be used to present animated visualizations and to calculate the volume enclosed. Accuracies up to 97 per cent have been reported, but performance is very much a function of the anatomy being measured, the probe trajectory, the segmentation and volume estimation algorithms, and any tissue motion during the scanning process. A comprehensive review has recently been provided by Noble and Boukerroui [**76**].

6 CLINICAL APPLICATIONS

There is a substantial literature on the clinical applications of 3D ultrasound. Most of these applications relate to the use of mechanically swept probes or 2D transducer arrays. For freehand 3D ultrasound, the practical inconvenience of the position sensor appears to have limited its exploitation primarily to two types of task: first, where it is necessary to locate the data in a fixed external coordinate system such as surgery or radiotherapy planning [**61**, **62**]; second, for the examination of long and complex structures which will not fit in a single sweep of the probe [**63**].

The tentative general reviews of the 1990s [**80**, **81**] have now given way to a deluge of reported applications and review articles covering the complete spectrum of medical practice (Fig. 13). Table 2 is designed to convey the considerable breadth and scale of current applications reported in the literature. The most common benefit derived from the use of 3D ultrasound rather than 2D ultrasound is an improved ability to visualize complex 3D structures. Examples of this can be found in gynaecological, neck, anorectal, skin, kidney, and brain imaging. The ability to locate particular features in an external coordinate system is used in brain, breast, liver, prostate, and spine imaging. Volume measurement is important in cardiac, fetal, and kidney work. Echocardiography often requires special stroboscopic scanning techniques to produce 3D information sufficiently quickly. Once acquired, the 3D data of the heart in motion are much easier to analyse and use for volume measurement than slices of 2D data. Doppler studies are used for blood vessels, and also for fetal, gynaecological, and kidney diagnosis.

Yet, for all this literature, most hospitals use almost entirely 2D ultrasound, with 3D only employed in a minority of applications. The enthusiastic burgeoning of research and innovative radiology is not yet fully reflected in day-to-day clinical practice. This presents an interesting contradiction that will be addressed in the next section.

7 FUTURE DEVELOPMENTS AND CONCLUSIONS

In the short term, the application of 3D ultrasound is expected gradually to increase. Apart for straightforward diagnostic visualization [**82**] it is used to support interventions such as image-guided surgery [**348**], ultrasound-guided radiotherapy planning [**349**], and image-guided biopsy [**268**, **350**]. There are a few technical barriers to increased usage in these areas. For example it is sometimes difficult to see fine biopsy needles in ultrasound images. If the ultrasound resolution was improved, or the needle material was developed with better backscatter properties, then the application would develop at a faster rate. However, there are also procedural barriers to usage. Ultrasound may not be used in surgery simply because the surgeon does not know how to scan and it is inconvenient to have a radiologist present in the operating theatre.

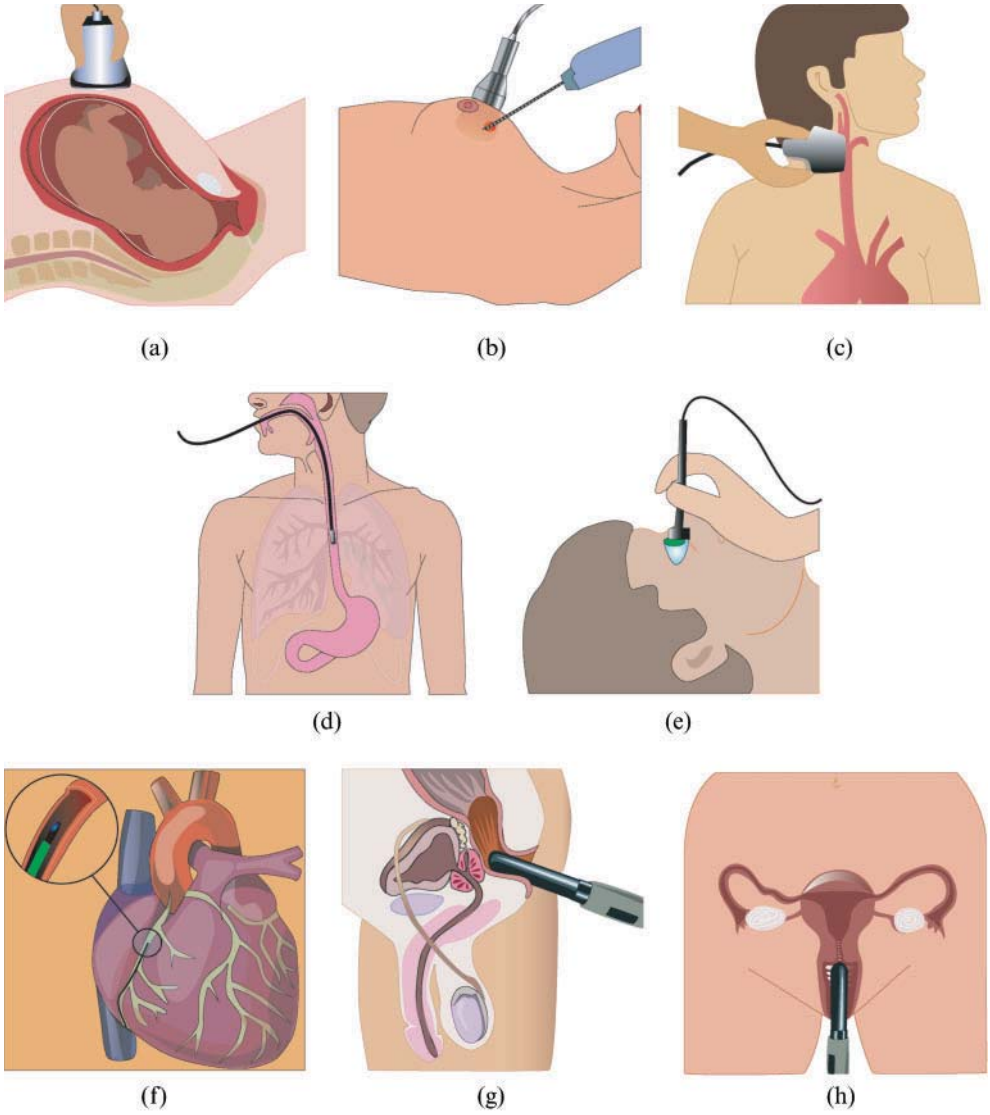

Fig. 13 3D ultrasound scanning methods used in clinical applications: (a) fetal screening; (b) ultrasound-guided breast biopsy; (c) carotid artery screening; (d) endoscopic probe used to scan the intestine; (e) eye scan; (f) intravascular ultrasound; (g) trans-rectal probe to scan the prostate; (h) trans-vaginal probe for gynaecological screening. See Table 2 for examples

However, what about the longer-term development of the field? Is it a natural and inevitable progression that 3D ultrasound will replace 2D ultrasound, or is real-time 2D ultrasound (perhaps with better elevational focusing), the most useful way in which ultrasound can be used in a clinical context?

Imagine a low-cost ultrasound machine with a 3D probe with most of the beam-forming circuitry built on to the back of a dense 2D transducer array. Suppose that it could produce fast, densely sampled volumes at better resolution than is currently available in a B-scan from a top-end machine. As each 3D data block is acquired, it will be registered with and assimilated into an overall data set. Clinicians will be able to navigate this rich block of dense data both during and after the recording session leading to increased efficiency and reliability [**351**, **352**]. Such a scenario could be possible, but it will take some time to come about. First, 2D transducer array technology has to mature; then the development costs have to be paid back and it has to become sufficiently common to drive the price down.

Although 3D ultrasound is important, it is not the most important factor. The key benefits of ultrasound are that it is inexpensive, safe, portable, and high resolution. Freehand 3D ultrasound has been

Table 2 Clinical applications of 3D ultrasound reported in the literature

Category	References
General surveys	[**10**, **80**–**92**]
Cardiac imaging (see Fig. 13(f))	Volume measurement [**93**–**97**] Registration [**98**, **99**] Doppler [**97**] Geometric modelling [**93**, **100**, **101**] Image segmentation [**102**] Image guidance [**103**] Real-time visualization [**94**, **104**, **105**]
Carotid imaging (see Fig. 13(c))	Volume measurement [**7**, **8**, **106**–**114**] Image segmentation [**115**] Intravascular Ultrasound [**116**, **117**]
Aorta imaging	Segmentation [**118**] Doppler [**101**, **119**–**122**] Volume measurement [**119**, **121**, **122**] Intra-operative image guidance [**123**]
Fetal imaging (see Fig. 13(a))	Review [**97**, **124**–**126**] Prenatal diagnosis [**12**, **127**–**185**] Doppler [**155**, **186**–**189**] Volume measurement [**140**, **144**, **145**, **147**, **154**, **169**, **190**–**200**] Geometric modelling [**78**, **92**, **201**–**203**]
Gynaecological imaging (see Fig. 13(h))	Surveys [**13**, **179**, **204**–**210**] Volume measurement [**211**–**222**] Anomaly diagnosis [**13**, **142**, **189**, **214**, **223**–**244**] Doppler [**189**, **222**, **227**, **233**, **241**, **243**, **245**–**249**] Image registration [**250**]
Bone imaging	Analysis [**251**] Image registration [**252**–**256**]
Neck imaging	Review [**257**] Diagnosis [**184**, **185**, **258**] Image registration [**259**]
Eye imaging (see Fig. 13(e))	Diagnosis [**260**–**262**]
Prostate imaging (see Fig. 13(g))	Diagnosis [**263**, **264**] Image segmentation [**265**] Image guidance [**106**, **266**–**268**] Geometric modelling [**92**]
Anorectal imaging (see Fig. 13(g))	Diagnosis [**269**, **270**]
Spine imaging	Motion analysis [**271**, **272**] Navigation [**273**] Image registration [**252**, **274**, **275**]
Skin imaging	Diagnosis [**276**–**278**]
Breast imaging (see Fig. 13(b))	Diagnosis [**279**–**281**] Image-guided biopsy [**106**, **282**–**284**] Image registration [**285**]
Kidney imaging	Volume measurement [**286**–**288**] Doppler [**289**, **290**] Surgical planning [**291**] Image registration [**292**] Geometric modelling [**96**]
Gastrointestinal imaging (see Fig. 13(d))	Review [**293**] Diagnosis [**294**–**304**]
Liver imaging	Navigation [**305**–**310**] Diagnosis [**311**] Intra-operative image guidance [**312**] Image registration [**45**, **313**] Geometric modelling [**92**]
Brain imaging	Neuro-navigation [**314**–**321**] Intra-operative image guidance [**322**–**328**] Image registration [**329**]
Gall-bladder imaging	Review [**330**] Diagnosis [**331**–**334**] Volume measurement [**5**, **331**]
Special-purpose imaging	Systems [**6**, **9**, **11**, **39**, **335**–**347**]

limited in its application because the external position sensor threatened the portability and ease of use. Mechanically swept probes and 2D transducer arrays have involved compromises in resolution and increases in price; hence they have been adopted at a slow rate. This explains the contrast between the enthusiasm of the research world and the apathy of front-line medicine that was described in the last section. 3D ultrasound will only become universal when it enhances rather than compromises ultrasound's key benefits. 2D transducer arrays, when they are dense enough, may offer improved focusing by working completely in three dimensions and may also reduce scan times. The flexibility to dissociate acquisition and reporting, as in other imaging modalities, may reduce costs. The richness and redundancy in 3D data may reduce the amount of training required for sonographers and radiologists while increasing their reliability. If the equipment is cheap enough, this deskilling could enable ultrasound to be used as a simple diagnostic tool in doctors' offices, removing the need for an expensive referral to the hospital.

However, this vision is a long way off, and the time that it will take to arrive is a function of both academic endeavour and commercial development. Over the last 10 years, the industrial landscape for ultrasound has changed. Now there are three major players in the west, a few more in Japan, and a small number of more specialist manufacturers. The main market is dominated by large corporations in which technical innovation does not necessarily equate with the sort of commercial gain that constitutes the primary business goal. There are therefore several ways in which change can come about. Perhaps the large corporations will lead the way because they have well-resourced multi-disciplinary research laboratories. Perhaps a tiny company will achieve a combination of technical and commercial flexibility which will enable it to grow rapidly and overtake the current leaders, much as Microsoft challenged IBM. Perhaps the fact that the large Japanese manufacturers have retained their technical and commercial independence over many years will give them a competitive advantage. Whatever route is taken, ultrasound in the next 20 years promises to be just as interesting and exciting as it was in the last 20 years.

ACKNOWLEDGEMENTS

The authors wish to thank Ms Norma Umer for drawing the diagrams for Figs 13 and 5, Professore B. (Pierre) T. Khuri-Yakub for permission to reproduce Fig. 4, Martha Morgan of Little Sprout Imaging for permission to reproduce Fig. 3, and GE Healthcare for permission to reproduce Fig. 9. Umer Zeeshan Ijaz is supported by the UK Engineering and Physical Sciences Research Council (Grant EP/F016476/1).

REFERENCES

1 **York, G.** and **Kim, Y.** Ultrasound processing and computing: review and future directions. *A. Rev. Biomed. Engng*, 1999, **1**, 559–588.
2 **Gee, A. H., Prager, R. W., Treece, G. M., Cash, C. J. C.,** and **Berman, L. H.** Processing and visualising three-dimensional ultrasound data. *Br. J. Radiol.*, 2004, **77**(S2), S186–S193.
3 **Nelson, T. R.** and **Pretorius, D. H.** Three-dimensional ultrasound imaging. *Ultrasound Med. Biol.*, 1998, **24**(9), 1243–1270.
4 **Fenster, A., Downey, D.,** and **Cardinal, H. N.** Three-dimensional ultrasound imaging. *Phys. Med. Biol.*, 2001, **46**, R67–R99.
5 **Pauletzki, J., Sackmann, M., Holl, J.,** and **Paumgartner, G.** Evaluation of gallbladder volume and emptying with a novel three-dimensional ultrasound system: comparison with the sum-of-cylinders and the ellipsoid methods. *J. Clin. Ultrasound*, 1996, **24**, 277–285.
6 **Boctor, E. M., Fischer, G., Choti, M. A., Fichtinger, G.,** and **Taylor, R. H.** A dual-armed robotic system for intraoperative ultrasound guided hepatic ablative therapy: a prospective study. In Proceedings of the 2004 IEEE International Conference on *Robotics and automation*, New Orleans, Louisiana, USA, April 2004, pp. 2517–2522 (IEEE, New York).
7 **Ainsworth, C. D., Blake, C. C., Tamayo, A., Beletsky, V., Fenster, A.,** and **Spence, J. D.** 3D ultrasound measurement of change in carotid plaque volume: A tool for rapid evaluation of new therapies. *Stroke*, 2005, **36**, 1904–1909.
8 **Fenster, A., Blake, C., Gyacskov, I., Landry, A.,** and **Spence, J. D.** 3D ultrasound analysis of carotid plaque volume and surface morphology. *Ultrasonics*, 2006, **44**, e153–e157.
9 **Fenster, A., Surry, K. J. M., Mills, G. R.,** and **Downey, D. B.** 3D ultrasound guided breast biopsy system. *Ultrasonics*, 2004, **42**, 769–774.
10 **Hünerbein, M.** Endorectal ultrasound in rectal cancer. *Colorectal Dis.*, 2003, **5**, 402–405.
11 **Gemmeke, H.** and **Ruiter, N. V.** 3D ultrasound computer tomography for medical imaging. *Nucl. Instrum. Meth. Phys. Res. A*, 2007, **580**, 1057–1065.
12 **Correa, F. F., Lara, C., Bellver, J., Remohí, J., Pellicer, A.,** and **Serra, V.** Examination of the fetal brain by transabdominal three-dimensional ultrasound: potential for routine neurosonographic

studies. *Ultrasound Obstet. Gynecol.*, 2006, **27**, 503–508.

13 **Wu, M.-H., Hsu, C.-C.,** and **Huang, K.-E.** Detection of congenital Müllerian duct anomalies using three-dimensional ultrasound. *J. Clin. Ultrasound*, 1997, **25**(9), 487–492.

14 **Merz, E., Benoit, B., Blaas, H. G., Baba, K., Kratochwil, A., Nelson, T., Pretorius, D., Jurkovic, D., Chang, F. M.,** and **Lee, A.** Standardization of three-dimensional images in obstetrics and gynecology: consensus statement. *Ultrasound Obstet. Gynecol.*, 2007, **29**(6), 697–703.

15 **Woo, J.** From wired frames to 3D, a short history of Kretztechnik AG, Zipf, Austria, available from http://www.ob-ultrasound.net/kretztechnik.html. Accessed in June 2009.

16 **Chang, J. H., Yen, J. T.,** and **Shung, K. K.** High-speed digital scan converter for high-frequency ultrasound sector scanners. *Ultrasonics*, 2008, **48**(5), 444–452.

17 **Duan, Q., Homma, S.,** and **Laine, A. F.** Analysis of 4D ultrasound for dynamic measures of cardiac function. In Proceedings of the IEEE Ultrasonics Symposium, 2007, pp. 1492–1495 (IEEE, New York).

18 **Light, E. D., Angle, J. F.,** and **Smith, S. W.** Real-time 3-D ultrasound guidance of interventional devices. *IEEE Trans. Ultrasonics, Ferroelectrics, Frequency Control*, 2008, **55**(9), 2066–2078.

19 **Erikson, K., Hairston, A., Nicoli, A., Stockwell, J.,** and **White, T.** 128×128 ultrasonic transducer hybrid array. In Proceedings of the IEEE Ultrasonics Symposium, 1997, pp. 1625–1627 (IEEE, New York).

20 **Smith, S. W., Pavy, H. G.,** and **von Ramm, O. T.** High-speed ultrasound volumetric imaging system – 1: transducer design and beam steering. *IEEE Trans. Ultrasonics Ferroelectrics Frequency Control*, 1991, **38**(2), 100–108.

21 **Light, E. D., Davidsen, R. E., Fiering, J. O., Hruschka, T. A.,** and **Smith, S. W.** Progress in two-dimensional arrays for real-time volumetric imaging. *Ultrasonic Imaging*, 1998, **20**(1), 1–15.

22 **Smith, S. W., Chu, K., Idriss, S. F., Ivancevich, N. M., Light, E. D.,** and **Wolf, P. D.** Feasibility study: real-time 3-D ultrasound imaging of the brain. *Ultrasound Med. Biol.*, 2004, **30**(10), 1365–1371.

23 **Yen, J. T.** and **Smith, S. W.** Real-time rectilinear volumetric imaging using a periodic array. *Ultrasound Med. Biol.*, 2002, **28**(7), 923–931.

24 **Yen, J. T.** and **Smith, S. W.** Real-time rectilinear 3-D ultrasound using receive mode multiplexing. *IEEE Trans. Ultrasonics Ferroelectrics Frequency Control*, 2004, **51**(2), 216–226.

25 **Austeng, A.** and **Holm, S.** Sparse 2-D arrays for 3-D phased array imaging – design methods. *IEEE Trans. Ultrasonics Ferroelectrics Frequency Control*, 2002, **49**(8), 1073–1086.

26 **Kirkebø, J. E.** and **Austeng, A.** Improved beamforming using curved sparse 2D arrays in ultrasound. *Ultrasonics*, 2007, **46**(2), 119–128.

27 **Liu, W., Zagzebski, J. A., Hall, T. J., Madsen, E. L., Varghese, T., Kliewer, M. A., Panda, S., Lowery, C.,** and **Barnes, S.** Acoustic backscatter and effective scatterer size estimates using a 2D CMUT transducer. *Phys. Med. Biol.*, 2008, **53**, 4169–4183.

28 **Wygant, I. O., Jamal, N., Lee, H. J., Nikoozadeh, A., Zhuang, X., Oralkan, O., Ergun, A. S., Karaman, M.,** and **Khuri-Yakub, B. T.** An integrated circuit with transmit beamforming and parallel receive channels for 3D ultrasound imaging: testing and characterization. In Proceedings of the IEEE Ultrasonics Symposium, 2007, pp. 25–28 (IEEE, New York).

29 **Wygant, I. O., Zhuang, X., Yeh, D. T., Oralkan, O., Ergun, A. S., Karaman, M.,** and **Khuri-Yakub, B. T.** Integration of 2D CMUT arrays with front-end electronics for volumetric ultrasound imaging. *IEEE Trans. Ultrasonics Ferroelectrics Frequency Control*, 2008, **55**(2), 327–342.

30 **Huang, Y., Zhuang, X., Haeggstrom, E. O., Ergun, A. S., Cheng, C. H.,** and **Khuri-Yakub, B. T.** Capacitative micromachined ultrasonic transducers (CMUTs) with isolation posts. *Ultrasonics*, 2008, **48**(1), 74–81.

31 **Bavaro, V., Caliano, G.,** and **Pappalardo, M.** Element shape design of 2-D CMUT arrays for reducing grating lobes. *IEEE Trans. Ultrasonics Ferroelectrics Frequency Control*, 2008, **55**(2), 308–318.

32 **Daft, C., Brueske, D., Wagner, P.,** and **Liu, D.** A matrix transducer design with improved image quality and acquisition rate. In Proceedings of the IEEE Ultrasonics Symposium, 2007, pp. 411–415 (IEEE, New York).

33 **Pursley, D.** Medical marvel. *New Electronics*, 2008, **41**(22), 46–48.

34 **Duric, N., Littrup, P., Poulo, L., Babkin, A., Pevzner, R., Holsapple, E., Rama, O.,** and **Glide, C.** Detection of breast cancer with ultrasound tomography: first results with the computerized ultrasound risk evaluation (CURE) prototype. *Med. Phys.*, 2007, **34**(2), 773–785.

35 **Glide-Hurst, C. K., Duric, N.,** and **Littrup, P.** Volumetric breast density evaluation from ultrasound tomography images. *Med. Phys.*, 2008, **35**(9), 3988–3997.

36 **Li, C., Huang, L., Duric, N., Zhang, H.,** and **Rowe, C.** An improved automatic time-of-flight picker for medical ultrasound tomography. *Ultrasonics*, 2009, **49**(1), 61–72.

37 **Gee, A. H., Prager, R. W., Treece, G. M.,** and **Berman, L. H.** Engineering a freehand 3D ultrasound system. *Pattern Recognition Lett.*, 2003, **24**(4–5), 757–777.

38 **Barratt, D. C., Ariff, B. B., Davies, A. H., Hughes, A. D., Thom, S. A. McG.,** and **Humphries, K. N. N.** Accuracy of three-dimensional ultrasound reconstruction in a clinical environment. *Ultrasound Med. Biol.*, 2000, **26**(Suppl. 2), A66.

39 **Welch, J. N., Johnson, J. A., Bax, M. R., Badr, R.,** and **Shahidi, R.** A real-time freehand 3D ultra-

sound system for image-guided surgery. In Proceedings of the IEEE Ultrasonics Symposium, 2000, Vol. 2, pp. 1601–1604 (IEEE, New York).

40 **Boctor, E. M., Choti, M. A., Burdette, E. C.,** and **Webster III, R. J.** Three-dimensional ultrasound-guided robotic needle placement: an experimental evaluation. *Int. J. Med. Robotics Comput. Assisted Surg.*, 2008, **4**(2), 180–191.

41 **Treece, G. M., Prager, R. W., Gee, A. H.,** and **Berman, L.** 3D ultrasound measurement of large organ volume. *Med. Image Analysis*, 2001, **5**(1), 41–54.

42 **Hummel, J., Figl, M., Bax, M., Bergmann, H.,** and **Birkfellner, W.** 2D/3D registration of endoscopic ultrasound to CT volume data. *Phys. Med. Biol.*, 2008, **53**(16), 4303–4316.

43 **Hastenteufel, M., Vetter, M., Meinzer, H.-P.,** and **Wolf, I.** Effect of 3D ultrasound probes on the accuracy of electromagnetic tracking systems. *Ultrasound Med. Biol.*, 2006, **32**(9), 1359–1368.

44 **Sheehan, F. H., Schneider, M., Bolson, E. L.,** and **Webster, B.** Tracking three dimensional ultrasound with immunity from ferro-magnetic interference. In Proceedings of the Sixth International Conference on *Medical image computing and computer-assisted intervention (MICCAI 2003)*, Lecture Notes in Computer Science, Vol. 2879, Montréal, Canada, 15–18 November 2003, pp. 192–198 (Springer-Verlag, Berlin).

45 **Cash, C. J. C., Berman, L. H., Treece, G. M., Gee, A. H.,** and **Prager, R. W.** Two- and three-dimensional ultrasound in the development of a needle-free injection system. *Br. J. Radiol.*, 2004, **77**, 236–242.

46 **Penney, G. P., Blackall, J. M., Hamady, M. S., Sabharwal, T., Adam, A.,** and **Hawkes, D. J.** Registration of freehand 3D ultrasound and magnetic resonance liver images. *Med. Image Analysis*, 2004, **8**(1), 81–91.

47 **Birkfellner, W., Watzinger, F., Wanschitz, F., Enislidis, G., Kollmann, C., Rafolt, D., Nowotny, R., Ewers, R.,** and **Bergmann, H.** Systematic distortions in magnetic position digitizers. *Med. Phys.*, 1998, **25**(11), 2242–2248.

48 **Birkfellner, W., Watzinger, F., Wanschitz, F., Ewers, R.,** and **Bergmann, H.** Calibration of tracking systems in a surgical environment. *IEEE Trans. Med. Imaging*, 1998, **17**(5), 737–742.

49 **Poulsen, C., Pedersen, P. C.,** and **Szabo, T. L.** An optical registration method for 3D ultrasound freehand scanning. In Proceedings of the IEEE Ultrasonics Symposium, 2005, pp. 1236–1240 (IEEE, New York).

50 **Goldsmith, A. M., Pedersen, P. C.,** and **Szabo, T. L.** An inertial-optical tracking system for portable, quantitative 3D ultrasound. In Proceedings of the IEEE Ultrasonics Symposium (*IUS 2008*), Beijing, People's Republic of China, 2–5 November, 2008, pp. 45–49 (IEEE, New York).

51 **Housden, R., Gee, A., Treece, G.,** and **Prager, R.** Sensorless reconstruction of unconstrained freehand 3D ultrasound data. *Ultrasound Med. Biol.*, 2007, **33**(3), 408–419.

52 **Hsu, P. W., Prager, R. W., Gee, A. H.,** and **Treece, G. M.** Freehand 3D ultrasound calibration: a review. In *Advanced imaging in biology and medicine* (Eds C. W. Sensen and B. Hallgrimsson), 2008, ch. 3, pp. 47–84 (Springer-Verlag, Berlin).

53 **Rousseau, F., Hellier, P.,** and **Barillot, C.** A novel temporal calibration method for 3-D ultrasound. *IEEE Trans. Med. Imaging*, 2006, **25**(8), 1108–1112.

54 **Hsu, P. W., Prager, R. W., Gee, A. H.,** and **Treece, G. M.** Real-time freehand 3D ultrasound calibration. *Ultrasound Med. Biol.*, 2008, **34**(2), 239–251.

55 **Treece, G. M., Lindop, J. E., Gee, A. H.,** and **Prager, R. W.** Freehand elastography with a 3D probe. *Ultrasound Med. Biol.*, 2008, **34**(3), 463–474. DOI:10.1016/j.ultrasmedbio.2007.08.014.

56 **Prager, R. W., Gee, A. H., Treece, G. M., Kingsbury, N. G., Lindop, J. E., Gomersall, H.,** and **Shin, H.-C.** Deconvolution and elastography based on three-dimensional ultrasound. In Proceedings of the IEEE International Ultrasonics Symposium (*IUS 2008*), Beijing, People's Republic of China, 2–5 November 2008, pp. 548–557.

57 **Kelly, I. M., Gardener, J. E., Brett, A. D., Richards, R.,** and **Lees, W. R.** 3-dimensional US of the fetus – work-in-progress. *Radiology*, 1994, **192**(1), 253–259.

58 **Solberg, O. V., Lindseth, F., Torp, H., Blake, R. E.,** and **Nagelhus Hernes, T. A.** Freehand 3D ultrasound reconstruction algorithms – a review. *Ultrasound Med. Biol.*, 2007, **33**(7), 991–1009.

59 **Prager, R. W., Gee, A. H., Treece, G. M.,** and **Berman, L. H.** Freehand 3D ultrasound without voxels: volume measurement and visualisation using the stradx system. *Ultrasonics*, 2002, **40**(1–8), 109–115.

60 University of Cambridge, Department of Engineering, Free software from the Medical Imaging Group, available from http://mi.eng.cam.ac.uk/~rwp/Software.html.

61 **Coles, C. E., Cash, C. J. C., Treece, G. M., Miller, F. N. A. C., Hoole, A. C. F., Gee, A. H., Prager, R. W., Sinnatamby, R., Britton, P., Wilkinson, J. S., Purushotham, A. D.,** and **Burnet, N. G.** High definition three-dimensional ultrasound to localise the tumour bed: a breast radiotherapy planning study. *Radiotherapy Oncol.*, 2007, **84**(3), 233–241.

62 **Cash, C. J. C., Coles, C. E., Treece, G. M., Purushotham, A. D., Britton, P., Sinnatamby, R., Gee, A. H.,** and **Prager, R. W.** Breast cancers: noninvasive method of preoperative localization with three-dimensional US and surface contour mapping. *Radiology*, 2007, **245**(2), 556–566. DOI:10.1148/radiol.2452000900.

63 **Cash, C., Sardesai, A., Berman, L., Herrick, G., Treece, G., Prager, R.,** and **Gee, A.** Spatial mapping of the brachial plexus using three-dimensional ultrasound. *Br. J. Radiol.*, 2005, **78**(936), 1086–1094.

64 **Nelson, T. R., Pretorius, D. H., Hull, A., Riccabona, M., Sklansky, M. S.,** and **James, G.** Sources and impact of artifacts on clinical three-dimensional ultrasound imaging. *Ultrasound Obstet. Gynecol.*, 2000, **16**(4), 374–383.

65 **Huang, J., Triedman, J. K., Vasilyev, N. V., Suematsu, Y., Cleveland, R. O.,** and **Dupont, P. E.** Imaging artifacts of medical instruments in ultrasound-guided interventions. *J. Ultrasound Med.*, 2007, **26**(10), 1303–1322.

66 **Robb, R. A.** Visualization in biomedical computing. *Parallel Comput.*, 1999, **25**(13–14), 2067–2110.

67 **Kuo, J., Bredthauer, G. R., Castellucci, J. B.,** and **von Ramm, O. T.** Interactive volume rendering of real-time three-dimensional ultrasound images. *IEEE Trans. Ultrasonics Ferroelectrics Frequency Control*, 2007, **54**(2), 313–318.

68 **Ropinski, T., Petkov, B., Fabritz, L.,** and **Hinrichs, K.** Small-animal ultrasound imaging – interactive reconstruction and visualisation of dynamic 3D ultrasound data sets. In Proceedings of the Third International Conference on *Computer graphics, theory and applications* (GRAPP 2008), Funchal, Portugal, 22–25 January 2008, pp. 308–315.

69 **Raine-Fenning, N., Campbell, B., Collier, J., Brincat, M.,** and **Johnson, I.** The reproducibility of endometrial volume acquisition and measurement with the vocal-imaging program. *Ultrasound Obstet. Gynecol.*, 2002, **19**(1), 69–75.

70 **Wang, Y., Cardinal, H. N., Downey, D. B.,** and **Fenster, A.** Semiautomatic three-dimensional segmentation of the prostate using two-dimensional ultrasound images. *Med. Phys.*, 2003, **30**(5), 887–897.

71 **Kot, B. C. W., Sin, D. M. H.,** and **Ying, M.** Evaluation of the accuracy and reliability of two 3-dimensional sonography methods in volume measurement of small structures: an *in vitro* phantom study. *J. Clin. Ultrasound*, 2009, **37**(2), 82–88.

72 **Treece, G. M., Prager, R. W., Gee, A. H.,** and **Berman, L.** Fast surface and volume estimation from non-parallel cross-sections, for freehand 3-D ultrasound. *Med. Image Analysis*, 1999, **3**(2), 141–173.

73 **Fenster, A.** and **Downey, D. B.** Three-dimensional ultrasound imaging and its use in quantifying organ and pathology volumes. *Analy. Bioanalyt. Chem.*, 2003, **377**(6), 982–989.

74 **Dydenko, I., Friboulet, D., Gorce, J.-M., D'Hooge, J., Bijnens, B.,** and **Magnin, I. E.** Towards ultrasound cardiac image segmentation based on the radiofrequency signal. *Med. Image Analysis*, 2003, **7**(3), 353–367.

75 **Castellano, G., Bonilha, L., Li, L. M.,** and **Cendes, F.** Texture analysis of medical images. *Clin. Radiol.*, 2004, **59**(12), 1061–1069.

76 **Noble, J. A.** and **Boukerroui, D.** Ultrasound image segmentation: a survey. *IEEE Trans. Med. Imaging*, 2006, **25**(8), 987–1010.

77 **Slabaugh, G., Unal, G., Wels, M., Fang, T.,** and **Rao, B.** Statistical region-based segmentation of ultrasound images. *Ultrasound Med. Biol.*, 2009, **35**(5), 781–795.

78 **Kalache, K. D., Espinoza, J., Chaiworapongsa, T., Londono, J., Schoen, M. L., Treadwell, M. C., Lee, W.,** and **Romero, R.** Three-dimensional ultrasound fetal lung volume measurement: A systematic study comparing the multiplanar method with the rotational (VOCAL) technique. *Ultrasound Obstet. Gynecol.*, 2003, **21**(2), 111–118.

79 **Raine-Fenning, N., Jayaprakasan, K., Clewes, J., Joergner, I., Dehghani Bonaki, S., Chamberlain, S., Devlin, L., Priddle, H.,** and **Johnson, I.** SonoAVC: A novel method of automatic volume calculation. *Ultrasound Obstet. Gynecol.*, 2008, **31**(6), 691–696.

80 **Hamper, U. M., Trapanotto, V., Sheth, S., Dejong, M. R.,** and **Caskey, C. I.** Three-dimensional US: preliminary clinical experience. *Radiology*, 1994, **191**(2), 397–401.

81 **Downey, D., Fenster, A.,** and **Williams, J. C.** Clinical utility of three-dimensional US. *Radiographics*, 2000, **20**, 559–571.

82 **Kim, S. H.** and **Choi, B. I.** Three-dimensional and four-dimensional ultrasound: techniques and abdominal applications. *J. Med. Ultrasound*, 2007, **15**(4), 228–242.

83 **Pretorius, D. H.** and **Nelson, T. R.** Three-dimensional ultrasound imaging in patient diagnosis and management: the future. *Ultrasound Obstet. Gynecol.*, 1991, **1**, 381–383.

84 **Forsberg, F., Rawool, N. M., Merton, D. A., Liu, J. B.,** and **Goldberg, B. B.** Contrast enhanced vascular three-dimensional ultrasound imaging. *Ultrasonics*, 2002, **40**, 117–122.

85 **Bonilla-Musoles, F., Raga, F., Osborne, N. G.,** and **Blanes, J.** Control of intrauterine device insertion with three-dimensional ultrasound: is it the future? *J. Clin. Ultrasound*, 1996, **24**, 263–267.

86 **Timor-Tritsch, I. E.** and **Platt, L. D.** Three-dimensional ultrasound experience in obstetrics. *Curr. Opin. Obstet. Gynecol.*, 2002, **14**(6), 569–575.

87 **Wong, J. B., Gerscovich, E. O., Cronan, M. S.,** and **Seibert, J. A.** Accuracy and precision of *in vitro* volumetric measurements by three-dimensional sonography. *Investigative Radiol.*, 1996, **31**(1), 26–29.

88 **Deng, J.** Terminology of three-dimensional and four-dimensional ultrasound imaging of the fetal heart and other moving body parts. *Ultrasound Obstet. Gynecol.*, 2003, **22**, 336–344.

89 **Campani, R., Bottinelli, O., Calliada, F.,** and **Coscia, D.** The latest in ultrasound: three-dimensional imaging. Part II. *Eur. J. Radiol.*, 1998, **27**(Suppl. 2), S183–S187.

90 **Kupesic, S.** The present and future role of three-dimensional ultrasound in assisted conception. *Ultrasound Obstet. Gynecol.*, 1998, **18**(3), 191–194.

91 **Rankin, R. N., Fenster, A., Downey, D. B., Munk, P. L., Levin, M. F.,** and **Vellet, A. D.** Three-dimensional sonographic reconstruction: techniques and diagnostic applications. *Am. J. Roentgenol.*, 1993, **161**(4), 695–702.

92 **Linney, A. D.** and **Deng, J.** Three-dimensional morphometry in ultrasound. *Proc. IMechE, Part H: J. Engineering in Medicine*, 1999, **213**(H3), 235–245. DOI:10.1243/0954411991534942.

93 **Papademetris, X., Sinusas, A. J., Dione, D. P.,** and **Duncan, J. S.** 3D cardiac deformation from ultrasound images. In Proceedings of the Second International Conference on *Medical image computing and computer-assisted intervention (MICCAI 99)*, Lecture Notes in Computer Science, Vol. 1679, Cambridge, UK, 19–22 September 1999, pp. 420–429 (Springer-Verlag, Berlin).

94 **Shiota, T., Jones, M., Chikada, M., Fleishman, C. E., Castellucci, J. B., Cotter, B., DeMaria, A. N., von Ramm, O. T., Kisslo, J., Ryan, T.,** and **Sahn, D. J.** Real-time three-dimensional echocardiography for determining right ventricular stroke volume in an animal model of chronic right ventricular volume overload. *Circulation*, 1998, **97**, 1897–1900.

95 **Yaman, C., Sommergruber, M., Ebner, T., Pölz, W., Moser, M.,** and **Tews, G.** Reproducibility of transvaginal three-dimensional endometrial volume measurements during ovarian stimulation. *Human Reproduction*, 1999, **14**(10), 2604–2608.

96 **Mor-Avi, V., Sugeng, L.,** and **Lang, R. M.** Three-dimensional adult echocardiography: where the hidden dimension helps. *Current Cardiol. Rep.*, 2008, **10**(3), 218–225.

97 **Yagel, S., Cohen, S. M., Shapiro, I.,** and **Valsky, D. V.** 3D and 4D ultrasound in fetal cardiac scanning: a new look at the fetal heart. *Ultrasound Obstet. Gynecol.*, 2007, **29**, 81–95.

98 **Pieper, S., Weidenbach, M.,** and **Berlage, T.** Registration of 3D ultrasound images to surface models of the heart. In Proceedings of the Conference on *Interfaces to real and virtual worlds*, Montpellier, France, 1997, pp. 211–213.

99 **Huang, X., Hill, N. A., Ren, J., Guiraudon, G., Boughner, D.,** and **Peters, T. M.** Dynamic 3D ultrasound and MR image registration of the beating heart. In Proceedings of the Eighth International Conference on *Medical image computing and computer-assisted intervention (MICCAI 2005)*, Lecture Notes in Computer Science, Vol. 3750, Palm Springs, California, USA, 26–29 October 2005, Part II, pp. 171–178 (Springer-Verlag, Berlin).

100 **Stetten, G. D.** and **Drezek, R.** Active Fourier contour applied to real time 3D ultrasound of the heart. *Int. J. Image Graphics*, 2001, **1**(4), 647–658.

101 **Cheng, L. K., Sands, G. B., French, R. L., Withy, S. J., Wong, S. P., Legget, M. E., Smith, W. M.,** and **Pullan, A. J.** Rapid construction of a patient-specific torso model from 3D ultrasound for non-invasive imaging of cardiac electrophysiology. *Med. Biol. Engng Comput.*, 2005, **43**(3), 325–330.

102 **Montagnat, J., Delingette, H.,** and **Malandain, G.** Cylindrical echocardiographic image segmentation based on 3D deformable models. In Proceedings of the Second International Conference on *Medical image computing and computer-assisted intervention (MICCAI 99)*, Lecture Notes in Computer Science, Vol. 1679, Cambridge, UK, 19–22 September 1999, pp. 168–175 (Springer-Verlag, Berlin).

103 **Smith, S. W., Booi, R. C., Light, E. D., Merdes, C. L.,** and **Wolf, P. D.** Guidance of cardiac pacemaker leads using real time 3D ultrasound: feasibility studies. *Ultrasonic Imaging*, 2002, **24**(2), 119–128.

104 **Stetten, G. D., Ota, T., Ohazama, C. J., Fleishman, C., Castellucci, J., Oxaal, J., Ryan, T., Kisslo, J.,** and **von Ramm, O. T.** Real-time 3D ultrasound: a new look at the heart. *J. Cardiovascular Diagnosis Procedures*, 1998, **15**(2), 73–84.

105 **Correale, M., Ieva, R.,** and **Di Biase, M.** Real-time three-dimensional echocardiography: an update. *Eur. J. Internal Med.*, 2008, **19**, 241–248.

106 **Fenster, A., Surry, K., Smith, W., Gill, J.,** and **Downey, D.** 3D ultrasound imaging: applications in image-guided therapy and biopsy. *Comput. Graphics*, 2002, **26**, 557–568.

107 **Delcker, A.** and **Diener, H. C.** 3D ultrasound measurement of atherosclerotic plaque volume in carotid arteries. *Bildgebung*, 1994, **61**(2), 116–121.

108 **Sameshima, T., Futami, S., Morita, Y., Yokogami, K., Miyahara, S., Sameshima, Y., Goya, T.,** and **Wakisaka, S.** Clinical usefulness of and problems with three-dimensional CT angiography for the evaluation of arteriosclerotic stenosis of the carotid artery: comparison with conventional sonography, MRA, and ultrasound sonography. *Surg. Neurol.*, 1999, **51**(3), 301–308.

109 **Landry, A., Spence, J. D.,** and **Fenster, A.** Measurement of carotid plaque volume by 3-dimensional ultrasound. *Stroke*, 2004, **35**(4), 864–869.

110 **Delcker, A.** and **Diener, H. C.** Quantification of atherosclerotic plaques in carotid arteries by three-dimensional ultrasound. *Br. J. Radiol.*, 1994, **67**(799), 672–678.

111 **Landry, A., Spence, J. D.,** and **Fenster, A.** Quantification of carotid plaque volume measurements using 3D ultrasound imaging. *Ultrasound Med. Biol.*, 2005, **31**(6), 751–762.

112 **Schminke, U., Motsch, L., Griewing, B., Gaull, M.,** and **Kessler, C.** Three-dimensional power-mode ultrasound for quantification of the progression of carotid artery atherosclerosis. *J. Neurol.*, 2000, **247**, 106–111.

113 **Allott, C. P., Barry, C. D., Pickford, R.,** and **Waterton, J. C.** Volumetric assessment of carotid artery bifurcation using freehand-acquired, compound 3D ultrasound. *Br. J. Radiol.*, 1999, **72**, 289–292.

114 **Chiu, B., Egger, M., Spence, J. D., Parraga, G.,** and **Fenster, A.** Quantification of carotid arteries atherosclerosis using 3D ultrasound images and area-preserving flattened maps. In *Medical imaging 2008: physiology, function and structure from medical images*, Proceedings of the SPIE, Vol. 6916 (Eds X. P. Hu and A. V. Clough). San Diego, California, USA, February 2008, p. 691603 (SPIE, Bellingham, Washington).

115 **Gill, J. D., Ladak, H. M., Steinman, D. A.,** and **Fenster, A.** Development and evaluation of a semiautomatic 3D segmentation technique of the carotid arteries from 3D ultrasound images. In *Medical imaging 1999: image processing*, Proceedings of the SPIE, Vol. 3661 (Ed. K. M. Hanson), 1999, pp. 214–221 (SPIE, Bellingham, Washington).

116 **von Birgelen, C., Mintz, G. S., Nicosia, A., Foley, D. P., van der Giessen, W. J., Bruining, N., Airiian, S. G., Roelandt, J. R. T. C., de Feyter, P. J.,** and **Serruys, P. W.** Electrocardiogram-gated intravascular ultrasound image acquisition after coronary stent deployment facilitates on-line three-dimensional reconstruction and automated lumen quantification. *J.A.M. Coll. Cardial.*, 1997, **30**(2), 436–443.

117 **Sousa, J. E., Costa, M. A., Abizaid, A., Abizaid, A. S., Feres, F., Pinto, I. M. F., Seixas, A. C., Staico, R., Mattos, L. A., Sousa, A. G. M. R., Falotico, R., Jaeger, J., Popma, J. J.,** and **Serruys, P. W.** Lack of neointimal proliferation after implantation of sirolimus-coated stents in human coronary arteries: a quantitative angiography and three-dimensional intravascular ultrasound study. *Circulation*, 2001, **103**, 192–195.

118 **Krissian, K., Ellsmere, J., Vosburgh, K., Kikinis, R.,** and **Westin, C.-F.** Multiscale segmentation of the aorta in 3D ultrasound images. In Proceedings of the 25th Annual International Conference of the IEEE Engineering in Medicine and Biology Society, Cancun, Mexico, 17–21 September 2003, pp. 638–641 (IEEE, New York).

119 **Mehwald, P. S., Rusk, R. A., Mori, Y., Li, X.-N., Zetts, A. D., Jones, M.,** and **Sahn, D. J.** A validation study of aortic stroke volume using dynamic 4-dimensional color Doppler: an *in vivo* study. *J. Am. Soc. Echocardiogr.*, 2002, **15**(10), 1045–1050.

120 **Ishii, M., Jones, M., Shiota, T., Yamada, I., Sinclair, B., Heinrich, R. S., Yoganathan, A. P.,** and **Sahn, D. J.** Temporal variability of vena contracta and jet areas with color Doppler in aortic regurgitation: a chronic animal model study. *J. Am. Soc. Echocardiogr.*, 1998, **11**(11), 1064–1071.

121 **Irvine, T., Stetten, G. D., Sachdev, V., Zetts, A. D., Jones, M., Mori, Y., Ramsperger, C., Castellucci, J. B., Kenny, A., Panza, J. A., von Ramm, O. T.,** and **Sahn, D. J.** Quantification of aortic regurgitation by real-time 3-dimensional echocardiography in a chronic animal model: computation of aortic regurgitant volume as the difference between left and right ventricular stroke volumes. *J. Am. Soc. Echocardiogr.*, 2001, **14**(11), 1112–1118.

122 **Haugen, B. O., Berg, S., Brecke, K. M., Samstad, S. O., Skærpe, T., Slørdahl, S. A.,** and **Torp, H.** Measurement of volumetric mitral and aortic blood flow based on a new freehand three-dimensional colour flow imaging method: an *in vivo* validation. *Eur. J. Echocardiogr.*, 2000, **1**, 204–212.

123 **Sjølie, E., Kaspersen, J. H., Wesche, J., Lindseth, F.,** and **Hernes, T. A. N.** Minimal invasive abdominal surgery based on ultrasound vision, possible? In *CARS 2001: computer assisted radiology and surgery*, International Congress Series, Vol. 1230, 2001, pp. 38–43 (Elsevier, Amsterdam).

124 **Kurjak, A., Vecek, N., Hafner, T., Bozek, T., Funduk-Kurjak, B.,** and **Ujevic, B.** Prenatal diagnosis: what does four-dimensional ultrasound add? *J. Perinatal Med.*, 2002, **30**, 57–62.

125 **Kurjak, A., Miskovic, B., Andonotopo, W., Stanojevic, M., Azumendi, G.,** and **Vrcic, H.** How useful is 3D and 4D ultrasound in perinatal medicine? *J. Perinatal Med.*, 2007, **35**, 10–27.

126 **Sklansky, M.** New dimensions and directions in fetal cardiology. *Curr. Opinions Pediat.*, 2003, **15**(5), 463–471.

127 **Mangione, R., Lacombe, D., Carles, D., Guyon, F., Saura, R.,** and **Horovitz, J.** Craniofacial dysmorphology and three-dimensional ultrasound: a prospective study on practicability for prenatal diagnosis. *Prenatal Diagnosis*, 2003, **23**, 810–818.

128 **Peralta, C. F. A., Falcon, O., Wegrzyn, P., Faro, C.,** and **Nicolaides, K. H.** Assessment of the gap between the fetal nasal bones at 11 to 13 + 6 weeks of gestation by three-dimensional ultrasound. *Ultrasound Obstet. Gynecol.*, 2005, **25**, 464–467.

129 **Michailidis, G. D., Papageorgiou, P.,** and **Economides, D. L.** Assessment of fetal anatomy in the first trimester using two- and three-dimensional ultrasound. *Br. J. Radiol.*, 2002, **75**, 215–219.

130 **Merz, E.** Use of 3D ultrasound in prenatal diagnosis. *Ultraschall Med.*, 1995, **16**(4), 154–161.

131 **Meinel, K.** and **Guntermann, E.** Transparent 3-D ultrasound in fetal abnormalities. *Ultraschall Med.*, 1998, **19**(3), 120–125.

132 **Arzt, W., Tulzer, G.,** and **Aigner, M.** Realtime 3D sonography of the normal fetal heart-clinical evaluation. *Ultraschall Med.*, 2002, **23**(6), 388–391.

133 **Clementschitsch, G., Hasenöhrl, G., Steiner, H.,** and **Staudach, A.** Early diagnosis of a fetal skeletal dysplasia associated with increased nuchal translucency with 2D and 3D ultrasound. *Ultraschall Med.*, 2003, **24**(5), 349–352.

134 **Esh-Broder, E., Ushakov, F. B., Imbar, T.,** and **Yagel, S.** Application of free-hand three-dimensional echocardiography in the evaluation of fetal cardiac ejection fraction: a preliminary study. *Ultrasound Obstet. Gynecol.*, 2004, **23**, 546–551.

135 **Shih, J.-C., Shyu, M.-K., Chang, C.-Y., Lee, C.-N., Lin, G.-J., Chen, W.-H., Fan, Y.-T.,** and **Hsieh, F.-J.** Application of the surface rendering techni-

que of three-dimensional ultrasound in prenatal diagnosis and counselling of Klippel–Trenaunay–Weber syndrome. *Prenatal Diagnosis*, 1998, **18**, 298–302.

136 Merz, E., Weber, G., Bahlmann, F., and **Miric-Tesanic, D.** Application of transvaginal and abdominal three-dimensional ultrasound for detection of exclusion of malformations of the fetal face. *Ultrasound Obstet. Gynecol.*, 1997, **9**, 237–243.

137 Rembouskos, G., Cicero, S., Longo, D., Vandecruys, H., and **Nicolaides, K. H.** Assessment of the fetal nasal bone at 11–14 weeks of gestation by three-dimensional ultrasound. *Ultrasound Obstet. Gynecol.*, 2004, **23**, 232–236.

138 Benacerraf, B. R., Sadow, P. M., Barnewolt, C. E., Estroff, J. A., and **Benson, C.** Cleft of the secondary palate without cleft lip diagnosed with three-dimensional ultrasound and magnetic resonance imaging in a fetus with Fryns' syndrome. *Ultrasound Obstet. Gynecol.*, 2006, **27**, 566–570.

139 Pooh, R. K., Pooh, K., Nakagawa, Y., Nishida, S., and **Ohno, Y.** Clinical application of three-dimensional ultrasound in fetal brain assessment. *Croat. Med. J.*, 2001, **41**(3), 245–251.

140 Clementschitsch, G., Hasenöhrl, G., Schaffer, H., and **Steiner, H.** Comparison between two- and three-dimensional ultrasound measurements of nuchal translucency. *Ultrasound Obstet. Gynecol.*, 2001, **18**, 475–480.

141 Sepulveda, W., Munoz, H., and **Alcalde, J. L.** Conjoined twins in triplet pregnancy: early prenatal diagnosis with three-dimensional ultrasound and review of literature. *Ultrasound Obstet. Gynecol.*, 2003, **22**, 199–204.

142 Schild, R. L., Plath, H., Hofstaetter, C., and **Hansmann, M.** Diagnosis of a fetal mesoblastic nephroma by 3D-ultrasound. *Ultrasound Obstet. Gynecol.*, 2000, **15**, 533–536.

143 Scharf, A., Ghazwiny, M. F., Steinborn, A., Baier, P., and **Sohn, C.** Evaluation of two-dimensional versus three-dimensional ultrasound in obstetric disease: a prospective study. *Fetal Diagnosis Therapy*, 2001, **16**(6), 333–341.

144 Falcon, O., Peralta, C. F. A., Cavoretto, P., Faiola, S., and **Nicolaides, K. H.** Fetal trunk and head volume measured by three-dimensional ultrasound at 11+0 to 13+6 weeks of gestation in chromosomally normal pregnancies. *Ultrasound Obstet. Gynecol.*, 2005, **26**, 263–266.

145 Chang, C.-H., Yu, C.-H., Ko, H.-C., Chen, C.-L., and **Chang, F.-M.** Fetal upper arm volume in predicting intrauterine growth restriction: a three-dimensional ultrasound sound. *Ultrasound Med. Biol.*, 2005, **31**(11), 1435–1439.

146 Bhat, A. H., Corbett, V., Carpenter, N., Liu, N., Liu, R., Wu, A., Hopkins, G., Sohaey, R., Winkler, C., Sahn, C. S., Sovinsky, V., Li, X., and **Sahn, D. J.** Fetal ventricular mass determination on three-dimensional echocardiography: studies in normal fetuses and validation experiments. *Circulation*, 2004, **110**, 1054–1060.

147 Schild, R. L., Fimmers, R., and **Hansmann, M.** Fetal weight estimation by three-dimensional ultrasound. *Ultrasound Obstet. Gynecol.*, 2000, **16**, 445–452.

148 Roman, A. S., Monteagudo, A., Timor-Tritsch, I., and **Rebarber, A.** First-trimester diagnosis of sacrococcygeal teratoma: the role of three-dimensional ultrasound. *Ultrasound Obstet. Gynecol.*, 2004, **23**, 612–614.

149 Plasencia, W., Dagklis, T., Sotiriadis, A., Borenstein, M., and **Nicolaides, K. H.** Frontomaxillary facial angle at 11+0 to 13+6 weeks gestation — reproducibility of measurements. *Ultrasound Obstet. Gynecol.*, 2007, **29**, 18–21.

150 Bongain, A., Benoit, B., Ejnes, L., Lambert, J. C., and **Gillet, J. Y.** Harlequin fetus: three-dimensional sonographic findings and new diagnostic approach. *Ultrasound Obstet. Gynecol.*, 2002, **20**, 82–85.

151 Wang, P.-H., Chen, G.-D., and **Lin, L.-Y.** Image comparison of basic cardiac views between two- and three-dimensional ultrasound in normal fetuses in anterior spine positions. *Int. J. Cardiovascular Imaging*, 2002, **18**, 17–23.

152 Faro, C., Wegrzyn, P., Benoit, B., Chaoui, R., and **Nicolaides, K. H.** Metopic suture in fetuses with holoprosencephaly at 11+0 to 13+6 weeks of gestation. *Ultrasound Obstet. Gynecol.*, 2006, **27**, 162–166.

153 Wang, P.-H., Ying, T.-H., Wang, P.-C., Shih, I.-C., Lin, L.-Y., and **Chen, G.-D.** Obstetrical three-dimensional ultrasound in the visualization of the intracranial midline and corpus collosum of fetuses with cephalic position. *Prenatal Diagnosis*, 2000, **20**, 518–520.

154 Wegrzyn, P., Faro, C., Falcon, O., Peralta, C. F. A., and **Nicolaides, K. H.** Placental volume measured by three-dimensional ultrasound at 11 to 13+6 weeks of gestation: relation to chromosomal defects. *Ultrasound Obstet. Gynecol.*, 2005, **26**, 28–32.

155 Chen, P., Shih, C. J.-C., Shih, S.-L., Huang, J.-K., Huang, J.-P., Lin, Y.-H., and **Wang, W.** Prenatal diagnosis of cephalothoracopagus janiceps disymmetros using three-dimensional power Doppler ultrasound and magnetic resonace imaging. *Ultrasound Obstet. Gynecol.*, 2003, **22**, 299–304.

156 Bonilla-Musoles, F., Machado, L. E., Raga, F., Osborne, N. G., and **Bonilla Jr, F.** Prenatal diagnosis of sacrococcygeal teratomas by two- and three-dimensional ultrasound. *Ultrasound Obstet. Gynecol.*, 2002, **19**, 200–205.

157 Hafner, E., Bock, W., Zoder, G., Schuchter, K., Rosen, A., and **Plattner, M.** Prenatal diagnosis of unilateral megalencephaly by 2D and 3D ultrasound: a case report. *Prenatal Diagnosis*, 1999, **19**, 159–162.

158 Tonni, G., Centini, G., and **Rosignoli, L.** Prenatal screening for fetal face and clefting in a prospec-

tive study on low-risk population: can 3- and 4-dimensional ultrasound enhance visualization and detection rate? *Oral Surg., Oral Med., Oral Pathol., Oral Radiol. Endodontics*, 2005, **100**, 420–426.

159 **Peng, S. S., Hsu, W. C., Chou, H. C., Peng, S. S., Chen, L. K., Chang, Y. L.,** and **Hsieh, F. J.** Prenatal three-dimensional ultrasound and magnetic resonance imaging evaluation of a fetal oral tumor in preparation for the *ex-utero* intrapartum treatment (EXIT) procedure. *Ultrasound Obstet. Gynecol.*, 2005, **25**(1), 76–79.

160 **Kurjak, A., Pooh, R. K., Merce, L. T., Carrera, J. M., Salihagic-Kadic, A.,** and **Andonotopo, W.** Structural and functional early human development assessed by three-dimensional and four-dimensional sonography. *Fertility Sterility*, 2005, **84**(5), 1285–1299.

161 **Blaicher, W., Lee, A., Deutinger, J.,** and **Bernaschek, G.** Sirenomelia: early prenatal diagnosis with combined two- and three-dimensional sonography. *Ultrasound Obstet. Gynecol.*, 2001, **17**, 542–543.

162 **Sedgmen, B., McMahon, C., Cairns, D., Benzie, R. J.,** and **Woodfield, R. L.** The impact of two-dimensional versus three-dimensional ultrasound exposure on maternal–fetal attachment and maternal health behavior in pregnancy. *Ultrasound Obstet. Gynecol.*, 2006, **27**, 245–251.

163 **Devore, G. R., Polanco, B., Sklansky, M. S.,** and **Platt, L. D.** The 'spin' technique: a new method for examination of the fetal outflow tracts using three-dimensional ultrasound. *Ultrasound Obstet. Gynecol.*, 2004, **24**, 72–82.

164 **Michailidis, G. D., Papageorgiou, P., Morris, R. W.,** and **Economides, D. L.** The use of three-dimensional ultrasound for fetal gender determination in the first trimester. *Br. J. Radiol.*, 2003, **76**, 448–451.

165 **Benoit, B.** The value of three-dimensional ultrasonography in the screening of the fetal skeleton. *Child's Nervous System*, 2003, **19**, 403–409.

166 **Eppel, W., Worda, C., Frigo, P.,** and **Lee, A.** Three- versus two-dimensional ultrasound for nuchal translucency thickness measurements: comparison of feasibility and levels of agreement. *Prenatal Diagnosis*, 2001, **21**, 596–601.

167 **Jürgens, J.** and **Chaoui, R.** Three-dimensional multiplanar time–motion ultrasound or anatomical m-mode of the fetal heart: a new technique in fetal echocardiography. *Ultrasound Obstet. Gynecol.*, 2003, **21**, 119–123.

168 **Moeglin, D.** and **Benoit, B.** Three-dimensional sonographic aspects in the antenatal diagnosis of achondroplasia. *Ultrasound Obstet. Gynecol.*, 2001, **18**, 81–83.

169 **Stanojevic, M., Hafner, T.,** and **Kurjak, A.** Three-dimensional ultrasound – a useful imaging technique in the assessment of neonatal brain. *J. Perinatal Med.*, 2002, **30**(1), 74–83.

170 **Viora, E., Sciarrone, A., Bastonero, S., Errante, G., Botta, G.,** and **Campogrande, M.** Three-dimensional ultrasound evaluation of short-rib polydactyly syndrome type II in the second trimester: a case report. *Ultrasound Obstet. Gynecol.*, 2002, **19**, 88–91.

171 **Chen, C.-P., Shih, J.-C., Tzen, C.-Y.,** and **Wang, W.** Three-dimensional ultrasound in the evaluation of complex anomalies associated with fetal ventral midline defects. *Ultrasound Obstet. Gynecol.*, 2002, **19**, 102–104.

172 **Benoit, B.** and **Chaoui, R.** Three-dimensional ultrasound with maximal mode rendering: a novel technique for the diagnosis of bilateral or unilateral absence or hypoplasia of nasal bones in second-trimester screening for down syndrome. *Ultrasound Obstet. Gynecol.*, 2005, **25**, 19–24.

173 **Rotten, D.** and **Levaillant, J. M.** Two- and three-dimensional sonographic assessment of the fetal face 1: a systematic analysis of the normal face. *Ultrasound Obstet. Gynecol.*, 2004, **23**, 224–231.

174 **Campbell, S., Lees, C., Moscoso, G.,** and **Hall, P.** Ultrasound antenatal diagnosis of cleft palate by a new technique: the 3D 'reverse face' view. *Ultrasound Obstet. Gynecol.*, 2005, **25**, 12–18.

175 **Krakow, D., Williams III, J., Poehl, M., Rimoin, D. L.,** and **Platt, L. D.** Use of three-dimensional ultrasound imaging in the diagnosis of prenatal-onset skeletal dysplasias. *Ultrasound Obstet. Gynecol.*, 2003, **21**, 467–472.

176 **Merz, E., Miric-Tesanic, D.,** and **Welter, C.** Value of the electronic scalpel (cut mode) in the evaluation of the fetal face. *Ultrasound Obstet. Gynecol.*, 2000, **16**, 564–568.

177 **Wallny, T. A., Theuerkauf, I., Schild, R. L., Perlick, L.,** and **Bertelsbeck, D. S.** The three-dimensional ultrasound evaluation of the rotator cuff – and experimental study. *Eur. J. Ultrasound*, 2000, **11**, 135–141.

178 **Lee, A., Deutinger, J.,** and **Bernaschek, G.** Voluvision: three-dimensional ultrasound of fetal malformations. *Am. J. Obstet. Gynecol.*, 1994, **170**(5, Part I), 1312–1314.

179 **Steiner, H., Staudach, A., Spitzer, D.,** and **Schaffer, H.** Three-dimensional ultrasound in obstetrics and gynaecology: technique, possibilities and limitations. *Human Reproduction*, 1994, **9**(9), 1773–1778.

180 **Paladini, D.** and **Volpe, P.** Posterior fossa and vermian morphometry in the characterization of fetal cerebellar abnormalities: a prospective three-dimensional ultrasound study. *Ultrasound Obstet. Gynecol.*, 2006, **27**, 482–489.

181 **Schild, R. L., Holthaus, S., d'Alquen, J., Fimmers, R., Dorn, C., van der Ven, H.,** and **Hansmann, M.** Quantitative assessment of subendometrial blood flow by three-dimensional ultrasound is an important factor of implantation in an *in-vitro* fertilization programme. *Human Reproduction*, 2000, **15**(1), 89–94.

182 **Dikkeboom, C. M., Roelfsema, N. M., Van Adriechem, L. N. A.,** and **Wladimiroff, J. W.** The role of three-dimensional ultrasound in visualizing the fetal cranial sutures and fontanels during the second half of pregnancy. *Ultrasound Obstet. Gynecol.*, 2004, **24**, 412–416.

183 **Gilmore, J. H., Gerig, G., Specter, B., Charles, C., Wilber, J., Herzberg, B.,** and **Kliewer, M. A.** Neonatal cerebral ventricle volume: a comparison of 3D ultrasound and magnetic resonance imaging. *Ultrasound Med. Biol.*, 2001, **27**(8), 1143–1146.

184 **Hanaoka, U., Yanagihara, T., Tanaka, H.,** and **Hata, T.** Comparison of three-dimensional, two-dimensional and color Doppler ultrasound in predicting the presence of a nuchal cord at birth. *Ultrasound Obstet. Gynecol.*, 2002, **19**(5), 471–474.

185 **Bonilla-Musoles, F., Raga, F., Villalobos, A., Blanes, J.,** and **Osborne, N. G.** First-trimester neck abnormalities: three-dimensional evaluation. *J. Ultrasound Med.*, 1998, **17**(7), 419–425.

186 **Deng, J., Yates, R., Sullivan, I. D., McDonald, D., Linney, A. D., Lees, W. R., Anderson, R. H.,** and **Rodeck, C. H.** Dynamic three-dimensional color Doppler ultrasound of human fetal intracardiac flow. *Ultrasound Obstet. Gynecol.*, 2002, **20**, 131–136.

187 **Brekke, S., Tegnander, E., Torp, H. G.,** and **Eik-Nes, S. H.** Tissue Doppler gated (TDOG) dynamic three-dimensional ultrasound imaging of the fetal heart. *Ultrasound Obstet. Gynecol.*, 2004, **24**, 192–198.

188 **Pooh, R. K.** and **Pooh, K.** Transvaginal 3D and Doppler ultrasonography of the fetal brain. *Semin. Perinatol.*, 2001, **25**(1), 38–43.

189 **Chaoui, R., Kalache, K. D.,** and **Hartung, J.** Application of three-dimensional power Doppler ultrasound in prenatal diagnosis. *Ultrasound Obstet. Gynecol.*, 2001, **17**, 22–29.

190 **Abuhamad, A., Falkensammer, P., Reichartseder, F.,** and **Zhao, Y.** Automated retrieval of standard diagnostic fetal cardiac ultrasound planes in the second trimester of pregnancy: a prospective evaluation of software. *Ultrasound Obstet. Gynecol.*, 2008, **31**(1), 30–36.

191 **Raga, F., Bonilla-Musoles, F., Casañ, E. M., Klein, O.,** and **Bonilla, F.** Assessment of endometrial volume by three-dimensional ultrasound prior to embryo transfer: clues to endometrial receptivity. *Human Reproduction*, 1999, **14**(11), 2851–2854.

192 **Ruano, R., Martinovic, J., Dommergues, M., Aubry, M.-C., Dumez, Y.,** and **Benachi, A.** Accuracy of fetal lung volume assessed by three-dimensional sonography. *Ultrasound Obstet. Gynecol.*, 2005, **26**, 725–730.

193 **Schild, R. L., Wallny, T., Fimmers, R.,** and **Hansmann, M.** Fetal lumbar spine volumetry by three-dimensional ultrasound. *Ultrasound Obstet. Gynecol.*, 1999, **13**, 335–339.

194 **Peralta, C. F. A., Cavoretto, P., Csapo, B., Falcon, O.,** and **Nicolaides, K. H.** Lung and heart volumes by three-dimensional ultrasound in normal fetuses at 12–32 weeks gestation. *Ultrasound Obstet. Gynecol.*, 2006, **27**, 128–133.

195 **Gerards, F. A., Engels, M. A. J., Twisk, J. W. R.,** and **Van Vugt, J. M. G.** Normal fetal lung volume measured with three-dimensional ultrasound. *Ultrasound Obstet. Gynecol.*, 2006, **27**, 134–144.

196 **Aviram, R., Kamar Shpan, D., Markovitch, O., Fishman, A.,** and **Tepper, R.** Three-dimensional first trimester fetal volumetry: comparison with crown rump length. *Early Human Development*, 2004, **80**, 1–5.

197 **Roelfsema, N. M., Hop, W. C. J., Boito, S. M. E.,** and **Wladimiroff, J. W.** Three-dimensional sonographic measurement of normal fetal brain volume during the second half of pregnancy. *Am. J. Obstet. Gynecol.*, 2004, **190**, 275–280.

198 **Monteagudo, A., Timor-Tritsch, I. E.,** and **Mayberry, P.** Three-dimensional transvaginal neurosonography of the fetal brain: 'navigating' in the volume scan. *Ultrasound Obstet. Gynecol.*, 2000, **16**, 307–313.

199 **Blaas, H.-G. K., Taipale, P., Torp, H.,** and **Eik-nes, S. H.** Three-dimensional ultrasound volume calculations of human embryos and young fetuses: a study on the volumetry of compound structures and its reproducibility. *Ultrasound Obstet. Gynecol.*, 2006, **27**, 640–646.

200 **Guerra, F. A., Isla, A. I., Aguilar, R. C.,** and **Fritz, E. G.** Use of free-hand three-dimensional ultrasound software in the study of the fetal heart. *Ultrasound Obstet. Gynecol.*, 2000, **16**, 329–334.

201 **D'Urso, P. S.** and **Thompson, R. G.** Fetal biomodelling. *Aust. N.Z. J. Obstet. Gynaecol.*, 1998, **38**(2), 205–207.

202 **Blaas, H.-G., Eik-Nes, S. H.,** and **Berg, S.** *In-vivo* three-dimensional ultrasound reconstructions of embryos and early fetuses. *Lancet*, 1998, **352**, 1182–1186.

203 **Timor-Tritsch, I. E., Monteagudo, A.,** and **Mayberry, P.** Three-dimensional ultrasound evaluation of the fetal brain: the three horn view. *Ultrasound Obstet. Gynecol.*, 2000, **16**, 302–306.

204 **Feichtinger, W.** Transvaginal three-dimensional imaging. *Ultrasound Obstet. Gynecol.*, 1993, **3**, 375–378.

205 **Sohn, Ch., Stolz, W., Nuber, B., Hesse, A.,** and **Hornung, B.** Three-dimensional ultrasound diagnostics in gynecology and obstetrics. *Geburtshilfe Frauenheilkd*, 1991, **51**, 335–340.

206 **Steiner, H., Staudach, A., Spitzer, D., Graf, A. H.,** and **Wienerroither, H.** 3D-sonography provides new aspects in obstetrical and gynecological ultrasound. *Geburtshilfe Frauenheilkd*, 1993, **53**, 779–782.

207 **Steiner, H., Gregg, A., Bogner, G., Graf, A. H., Weiner, C. P.,** and **Staudach, A.** First trimester three-dimensional ultrasound volumetry of the gestational sac. *Arch. Gynecol. Obstet.*, 1993, **255**(4), 165–170.

208 **Gregg, A., Steiner, H., Staudach, A.,** and **Weiner, C. P.** Accuracy of 3D sonographic volume measurements. *Am. J. Obstet. Gynecol.*, 1993, **168**(Suppl.), 348–355.

209 **Kuo, H. C., Chang, F. M., Wu, C. H., Yao, B. L.,** and **Liu, C. H.** The primary application of three-dimensional ultrasonography in obstetrics. *Am. J. Obstet. Gynecol.*, 1992, **166**, 880–886.

210 **Nelson, T. R.** and **Pretorius, D. H.** Three-dimensional ultrasound of fetal surface features. *Ultrasound Obstet. Gynecol.*, 1992, **2**(3), 166–174.

211 **Chou, C.-Y., Hsu, K.-F., Wang, S.-T., Huang, S.-C., Tzeng, C.-C.,** and **Huang, K.-E.** Accuracy of three-dimensional ultrasonography in volume estimation of cervical carcinoma. *Gynecologic Oncol.*, 1997, **66**, 89–93.

212 **Yaman, C., Ebner, T., Jesacher, K., Obermayr, G., Pölz, W.,** and **Tews, G.** Reproducibility of three-dimensional ultrasound endometrial volume measurements in patients with postmenopausal bleeding. *Ultrasound Obstet. Gynecol.*, 2002, **19**, 282–286.

213 **Bordes, A., Bory, A. M., Benchaïb, M., RudiGroz, R. C.,** and **Salle, B.** Reproducibility of transvaginal three-dimensional endometrial volume measurements with virtual organ computer-aided analysis (vocal) during ovarian stimulation. *Ultrasound Obstet. Gynecol.*, 2002, **19**, 76–80.

214 **Nardo, L. G., Buckett, W. M.,** and **Khullar, V.** Determination of the best-fitting ultrasound formulaic method for ovarian volume measurement in women with polycystic ovary syndrome. *Fertility Sterility*, 2003, **79**(3), 632–633.

215 **Schild, R. L., Knobloch, C., Dorn, C., Fimmers, R., van der Ven, H.,** and **Hansmann, M.** The role of ovarian volume in an *in vitro* fertilization programme as assessed by 3D ultrasound. *Arch. Gynecol. Obstet.*, 2001, **265**, 67–72.

216 **Rempen, A.** The shape of the endometrium evaluated with three-dimensional ultrasound: an additional predictor of extrauterine pregnancy. *Human Reproduction*, 1998, **13**(2), 450–454.

217 **Nardo, L. G., Buckett, W. M., White, D., Digesu, A. G., Franks, S.,** and **Khullar, V.** Three-dimensional assessment of ultrasound features in women with clomiphene citrate-resistant polycystic ovarian syndrome (pcos): ovarian stromal volume does not correlate with biochemical indices. *Human Reproduction*, 2002, **17**(4), 1052–1055.

218 **Schild, R. L., Indefrei, D., Eschweiler, S., van der Ven, H., Fimmers, R.,** and **Hansmann, M.** Three-dimensional endometrial volume calculation and pregnancy rate in an *in-vitro* fertilization program. *Human Reproduction*, 1999, **14**(5), 1255–1258.

219 **Hoesli, I. M., Survek, D. V., Tercanli, S.,** and **Holzgreve, W.** Three dimensional volume measurement of the cervix during pregnancy compared to conventional 2D-sonography. *Int. J. Gynecol. Obstet.*, 1999, **64**, 115–119.

220 **Kyei-Mensah, A., Maconochie, N., Zaidi, J., Pittrof, R., Campbell, S.,** and **Tan, S. L.** Transvaginal three-dimensional ultrasound: reproducibility of ovarian and endometrial volume measurements. *Fertility Sterility*, 1996, **66**(5), 718–722.

221 **Dietz, H. P.** and **Wilson, P. D.** The 'iris effect': how two-dimensional and three-dimensional ultrasound can help us understand anti-incontinence procedures. *Ultrasound Obstet. Gynecol.*, 2004, **23**, 267–271.

222 **Jayaprakasan, K., Hopkisson, J. F., Campbell, B. K., Clewes, J., Johnson, I. R.,** and **Raine-Fenning, N. J.** Quantification of the effect of pituitary down-regulation on the 3D ultrasound predictors of ovarian response. *Human Reproduction*, 2008, **23**(7), 1538–1544.

223 **Dietz, H. P., Shek, C.,** and **Clarke, B.** Biometry of the pubovisceral muscle and levator hiatus by three-dimensional pelvic floor ultrasound. *Ultrasound Obstet. Gynecol.*, 2005, **25**, 580–585.

224 **ter Haar Romeny, B. M., Ttulaer, B., Kalitzin, S., Sheffer, G., Broekmans, F., Staal, J.,** and **te Velde, E.** Computer assisted human follicle analysis for fertility prospects with 3D ultrasound. In Proceedings of the 16th International Conference on *Information processing in medical imaging (IPMI '99)*, Lecture Notes in Computer Science, Vol. 1613, Visegrád, Hungary, 28 June–2 July 1999, pp. 55–69 (Springer-Verlag, Berlin).

225 **Robinson, D., Toozs-Hobson, P., Cardozo, L.,** and **Digesu, A.** Correlating structure and function: three-dimensional ultrasound of the urethral sphincter. *Ultrasound Obstet. Gynecol.*, 2004, **23**, 272–276.

226 **Jayaprakasan, K., Hilwah, N., Kendall, N. R., Hopkisson, J. F., Campbell, B. K., Johnson, I. R.,** and **Raine-Fenning, N. J.** Does 3D ultrasound offer any advantage in the pretreatment assessment of ovarian reserve and prediction of outcome after assisted reproduction treatment? *Human Reproduction*, 2007, **22**(7), 1932–1941.

227 **Testa, A. C., Ajossa, S., Ferrandina, G., Fruscella, E., Ludovisi, M., Malaggese, M., Scambia, G., Melis, G. B.,** and **Guerriero, S.** Does quantitative analysis of three-dimensional power Doppler angiography have a role in the diagnosis of malignant pelvic solid tumors? A preliminary study. *Ultrasound Obstet. Gynecol.*, 2005, **26**, 67–72.

228 **Bonilla-Musoles, F., Raga, F.,** and **Osborne, N. G.** Three-dimensional ultrasound evaluation of ovarian masses. *Gynecologic Oncol.*, 1995, **59**(1), 129–135.

229 **Chan, C. C. W., Ng, E. H. Y., Li, C. F.,** and **Ho, P. C.** Impaired ovarian blood flow and reduced antral follicle count following laparoscopic salpingectomy for ectopic pregnancy. *Human Reproduction*, 2003, **18**(10), 2175–2180.

230 **Dietz, H. P., Pang, S., Korda, A.,** and **Benness, C.** Paravaginal defects: a comparison of clinical examination and 2D/3D ultrasound imaging. *Aust. N.Z. J. Obstet. Gynaecol.*, 2005, **45**, 187–190.

231 **Dietz, H. P.** and **Steensma, A. B.** Posterior compartment prolapse on two-dimensional and three-dimensional pelvic floor ultrasound: the distinction between true rectocele, perineal hypermobility and enterocele. *Ultrasound Obstet. Gynecol.*, 2005, **26**, 73–77.

232 **Kupesic, S.** and **Kurjak, A.** Predictors of IVF outcome by three-dimensional ultrasound. *Human Reproduction*, 2002, **17**(4), 950–955.

233 **Pan, H.-A., Wu, M.-H., Cheng, Y.-C., Li, C.-H.,** and **Chang, F.-M.** Quantification of Doppler signal in polycystic ovary syndrome using three-dimensional power Doppler ultrasonography: a possible new marker for diagnosis. *Human Reproduction*, 2002, **17**(1), 201–206.

234 **Scheffer, G. J., Broekmans, F. J. M., Bancsi, L. F., Habbema, J. D. F., Looman, C. W. N.,** and **Te Velde, E. R.** Quantitative transvaginal two- and three-dimensional sonography of the ovaries: reproducibility of antral follicle counts. *Ultrasound Obstet. Gynecol.*, 2002, **20**, 270–275.

235 **Salim, R., Woelfer, B., Backos, M., Regan, L.,** and **Jurkovic, D.** Reproducibility of three-dimensional ultrasound diagnosis of congenital uterine anomalies. *Ultrasound Obstet. Gynecol.*, 2003, **21**, 578–582.

236 **Sylvestre, C., Child, T. J., Tulandi, T.,** and **Tan, S. L.** A prospective study to evaluate the efficacy of two- and three-dimensional sonohysterography in women with intrauterine lesions. *Fertility Sterility*, 2003, **79**(5), 1222–1225.

237 **Dietz, H. P.** Ultrasound imaging of the pelvic floor. Part II: three-dimensional or volumetric imaging. *Ultrasound Obstet. Gynecol.*, 2004, **23**, 615–625.

238 **Toozs-Hobson, P., Khullar, V.,** and **Cardozo, L.** Three-dimensional ultrasound: a novel technique for investigating the urethral sphincter in the third trimester of pregnancy. *Ultrasound Obstet. Gynecol.*, 2001, **17**, 421–424.

239 **Dietz, H. P., Steensma, A. B.,** and **Hastings, R.** Three-dimensional ultrasound imaging of the pelvic floor: the effect of parturition on paravaginal support structures. *Ultrasound Obstet. Gynecol.*, 2003, **21**, 585–595.

240 **Baba, K., Ishihara, O., Hayashi, N., Saitoh, M., Taya, J.,** and **Kinoshita, K.** Three-dimensional ultrasound in embryo transfer. *Ultrasound Obstet. Gynecol.*, 2000, **16**, 372–373.

241 **Schuchter, K., Metzenbauer, M., Hafner, E.,** and **Philipp, K.** Uterine artery Doppler and placental volume in the first trimester in the prediction of pregnancy complications. *Ultrasound Obstet. Gynecol.*, 2001, **18**, 590–592.

242 **Watermann, D., Denschlag, D., Hanjalic-Beck, A., Keck, C., Karck, U.,** and **Prömpeler, H.** Hystero-saplingo-contrast-sonography with 3-D-ultrasound – a pilot study. *Ultraschall Med.*, 2004, **25**(5), 367–372.

243 **Shih, J. C.** Cesarean scar pregnancy: diagnosis with three-dimensional (3D) ultrasound and 3D power Doppler. *Ultrasound Obstet. Gynecol.*, 2004, **23**, 306–307.

244 **Tseng, L.-H.** Ultrasound in urogynecology: an update on clinical application. *J. Med. Ultrasound*, 2007, **15**(1), 45–57.

245 **Ng, E. H. Y., Chan, C. C. W., Tang, O. S., Yeung, W. S. B.,** and **Ho, P. C.** The role of endometrial and subendometrial blood flows measured by three-dimensional power Doppler ultrasound in the prediction of pregnancy during IVF treatment. *Human Reproduction*, 2006, **21**(1), 164–170.

246 **Ng, E. H. Y., Chan, C. C. W., Tang, O. S., Yeung, W. S. B.,** and **Ho, P. C.** Endometrial and subendometrial blood flow measured by three-dimensional power Doppler ultrasound in patients with small intramural uterine fibroids during IVF treatment. *Human Reproduction*, 2005, **20**(2), 501–506.

247 **Raine-Fenning, N. J., Clewes, J. S., Kendall, N. R., Bunkheila, A. K., Campbell, B. K.,** and **Johnson, I. R.** The interobserver reliability and validity of volume circulation from three-dimensional ultrasound datasets in the *in vitro* setting. *Ultrasound Obstet. Gynecol.*, 2003, **21**, 283–291.

248 **Ng, E. H. Y., Chan, C. C. W., Tang, O. S.,** and **Ho, P. C.** Factors affecting endometrial and subendometrial blood flow measured by three-dimensional power Doppler ultrasound during IVF treatment. *Human Reproduction*, 2006, **21**(4), 1062–1069.

249 **Rovas, L., Sladkevicius, P., Strobel, E.,** and **Valentin, L.** Three-dimensional power Doppler ultrasound assessment of the cervix for the prediction of successful induction of labor with prostaglandin in prolonged pregnancy. *J. Ultrasound Med.*, 2005, **24**, 933–939.

250 **Verhey, J. F., Wisser, J., Warfield, S. K., Rexilius, J.,** and **Kikinis, R.** Non-rigid registration of a 3D ultrasound and a MR image data set of the female pelvic floor using a biomechanical model. *BioMed. Engng Online*, 2005, **4**, 19.

251 **Hünerbein, M., Raschke, M., Khodadadyan, C., Hohenberger, P., Haas, N. P.,** and **Schlag, P. M.** Three-dimensional ultrasonography of bone and soft tissue lesions. *Eur. J. Ultrasound*, 2001, **13**, 17–23.

252 **Moghari, M. H.** and **Abolmaesumi, P.** A novel incremental technique for ultrasound to CT bone surface registration using unscented Kalman filtering. In Proceedings of the Eighth International Conference on *Medical image computing and computer-assisted intervention (MICCAI 2005)*, Lecture Notes in Computer Science, Vol. 3750, Palm Springs, California, USA, 26–29 October 2005, Part II, pp. 197–204 (Springer-Verlag, Berlin).

253 **Brendel, B., Winter, S., Rick, A., Stockheim, M.,** and **Ermert, H.** Registration of 3D CT and ultrasound datasets of the spine using bone structures. *Comput. Aided Surg.*, 2002, **7**, 146–155.

254 **Winter, S., Brendel, B.,** and **Igel, C.** Registration of bone structures in 3D ultrasound and CT data:

comparison of different optimization strategies. In *CARS 2005: computer assisted radiology and surgery*, International Congress Series, Vol. 1281, 2005, pp. 242–247 (Elsevier, Amsterdam).

255 **Winter, S., Brendel, B., Rick, A., Stockheim, M., Schmieder, K.,** and **Ermert, H.** Registration of bone surfaces, extracted from CT-datasets, with 3D ultrasound. *Biomedizinische Technik*, 2002, **47**(Suppl. 1, Part 1), 57–60.

256 **Barratt, D. C., Penney, G. P., Chan, C. S. K., Slomczykowski, M., Carter, T. J., Edwards, P. J.,** and **Hawkes, D. J.** Self-calibrating 3D-ultrasound-based bone registration for minimally invasive orthopedic surgery. *IEEE Trans. Med. Imaging*, 2006, **25**(3), 312–323.

257 **Senchenkov, A.** and **Staren, E. D.** Ultrasound in head and neck surgery: thyroid, parathyroid, and cervical lymph nodes. *Surg. Clin. North Am.*, 2004, **84**(4), 973–1000.

258 **Klimek, L., Schreiber, J., Amedee, R. G.,** and **Mann, W. J.** Three-dimensional ultrasound evaluation in the head and neck. *Otolaryngol. – Head Neck Surg.*, 1998, **118**(2), 267–271.

259 **Wein, W., Röper, B.,** and **Navab, N.** Automatic registration and fusion of ultrasound with CT for radiotherapy. In Proceedings of the Eighth International Conference on *Medical image computing and computer-assisted intervention (MICCAI 2005)*, Lecture Notes in Computer Science Vol. 3750, Palm Springs, California, USA, 26–29 October 2005, Part II, pp. 303–311 (Springer-Verlag, Berlin).

260 **Finger, P. T., Khoobehi, A., Ponce-Contreras, M. R., Rocca, D. D.,** and **Garcia Jr, J. P. S.** Three dimensional ultrasound of retinoblastoma: initial experience. *Br. J. Opthalmol.*, 2002, **86**(10), 1136–1138.

261 **Romero, J. M., Finger, P. T., Rosen, R. B.,** and **Iezzi, R.** Three-dimensional ultrasound for the measurement of choroidal melanomas. *Arch. Opthalmol.*, 2001, **119**, 1275–1282.

262 **Stachs, O., Martin, H., Kirchhoff, A., Stave, J., Terwee, T.,** and **Guthoff, R.** Monitoring accommodative ciliary muscle function using three-dimensional ultrasound. *Graefe's Arch. Clin. Exp. Opthalmol.*, 2002, **240**(11), 906–912.

263 **Fenster, A., Tong, S., Cardinal, H. N., Blake, C.,** and **Downey, D. B.** Three-dimensional ultrasound imaging system for prostrate cancer diagnosis and treatment. *IEEE Instrum. Meas. Mag.*, 1996, **1**(4), 32–35.

264 **Fung, A. Y. C., Ayyangar, K. M., Djajaputra, D., Nehru, R. M.,** and **Enke, C. A.** Ultrasound-based guidance of intensity-modulated radiation therapy. *Med. Dosimetry*, 2006, **31**(1), 20–29.

265 **Hu, N., Downey, D. B., Fenster, A.,** and **Ladak, H. M.** Prostate boundary segmentation from 3D ultrasound images. *Med. Phys.*, 2003, **30**(7), 1648–1659.

266 **Chinnaiyan, P., Tomée, W., Patel, R., Chappell, R.,** and **Ritter, M.** 3D-ultrasound guided radiation therapy in the post-prostatectomy setting. *Technol. Cancer Res. Treatment*, 2003, **2**(5), 455–458.

267 **Lattanzi, J., McNeeley, S., Donnelly, S., Palacio, E., Hanlon, A., Schulteiss, T. E.,** and **Hanks, G. E.** Ultrasound-based stereotactic guidance in prostate cancer – quantification of organ motion and set-up errors in external beam radiation therapy. *Comput. Aided Surg.*, 2000, **5**(4), 289–295.

268 **Shen, F., Shinohara, K., Kumar, D., Khemka, A., Simineau, A. R., Werahera, P. N., Li, L., Guo, Y., Narayanan, R., Wei, L., Barqawi, A., Crawford, E. D., Davatzikos, C.,** and **Suri, J. S.** Three-dimensional sonography with needle tracking: role in diagnosis and treatment of prostate cancer. *J. Ultrasound Med.*, 2008, **27**(6), 895–905.

269 **Gravante, G.** and **Giordano, P.** The role of three-dimensional endoluminal ultrasound imaging in the evaluation of anorectal diseases: a review. *Surg. Endoscopy*, 2008, **22**, 1570–1578.

270 **Giovannini, M.** and **Ardizzone, S.** Anorectal ultrasound for neoplastic and inflammatory lesions. *Best Practice Res. Clin. Gastroentherol.*, 2006, **20**(1), 113–135.

271 **Natalis, M.** and **König, A.** Noninvasive, accurate and reliable measurement of cervical spine motion with a 3D real-time ultrasound motion analyzer. *Ultraschall Med.*, 1999, **20**(2), 70–73.

272 **Strimpakos, N., Sakellari, V., Gioftsos, G., Papathanasiou, M., Brountzos, E., Kelekis, D., Kapreli, E.,** and **Oldham, J.** Cervical spine ROM measurements: optimizing the testing protocol by using a 3D ultrasound-based motion analysis system. *Cephalagia*, 2005, **25**, 1133–1145.

273 **Bonsanto, M. M., Metzner, R., Aschoff, A., Tronnier, V., Kunze, S.,** and **Wirtz, C. R.** 3D ultrasound navigation in syrinx surgery – a feasibility study. *Acta Neurochir.*, 2005, **147**, 533–541.

274 **Firle, E. A., Wesarg, S., Karangelis, G.,** and **Dold, C.** Validation of 3D ultrasound: CT registration of prostate images. In *Photonic crystal materials and devices*, Proceedings of the SPIE, Vol. 5032 (Eds M. Sonka and J. M. Fitzpatrick), 2003, pp. 354–362 (SPIE, Bellingham, Washington).

275 **Winter, S., Brendel, B., Pechlivanis, I., Schmieder, K.,** and **Igel, C.** Registration of CT and intraoperative 3-D ultrasound images of the spine using evolutionary and gradient-based methods. *IEEE Trans. Evolutionary Comput.*, 2008, **12**(3), 284–296.

276 **Stücker, M., Wilmert, M., Hoffmann, K., El-Gammal, S., Dirting, K.,** and **Altmeyer, P.** Objectivity, reproducibility and validity of 3D ultrasound in dermatology. *Bildebung*, 1995, **62**(3), 179–188.

277 **Sahiner, B., LeCarpentier, G. L., Chan, H.-P., Roubidoux, M. A., Petrick, N., Goodsitt, M. M., Sanjay-Gopal, S.,** and **Carson, P. L.** Computerized characterization of breast masses using three-dimensional ultrasound images. In *Medical imaging 1998: PACS design and evaluation: engineer-*

ing and clinical issues, Proceedings of the SPIE, Vol. 3338 (Ed. K. M. Hanson), 1998, pp. 313–317 (SPIE, Bellingham, Washington).

278 Watermann, D. O., Földi, M., Hanjalic-Beck, A., Hasenburg, A., Lüghausen, A., Prömpeler, H., Gitsch, G., and **Stickeler, E.** Three-dimensional ultrasound for the assessment of breast lesions. *Ultrasound Obstet. Gynecol.*, 2005, **25**, 592–598.

279 Kotsianos, D., Wirth, S., Fischer, T., Hiltawsky, K., Sittek, H., and **Reiser, M.** 3D ultrasound (3D US) in the diagnosis of focal breast lesions. *Radiologe*, 2005, **45**(3), 237–244.

280 Rotten, D., Levaillant, J. M., Constancis, E., Billon, A. C., Le Guerinel, Y., and **Rua, P.** Three-dimensional imaging of solid breast tumors with ultrasound: preliminary data and analysis of its possible contribution to the understanding of the standard two-dimensional sonographic images. *Ultrasound Obstet. Gynecol.*, 1991, **1**, 384–390.

281 Weismann, C. F. and **Datz, L.** Diagnostic algorithm: how to make use of new 2D, 3D and 4D ultrasound technologies in breast imaging. *Eur. J. Radiol.*, 2007, **64**(2), 250–257.

282 Lell, M., Wenkel, E., Aichinger, U., Schulz-Wendtland, R., and **Bautz, W.** 3D ultrasound in core breast biopsy. *Ultraschall Med.*, 2004, **25**(2), 126–130.

283 Weismann, C. F., Forstner, R., Prokop, E., and **Rettenbacher, T.** Three-dimensional targeting: a new three-dimensional ultrasound technique to evaluate needle position during breast biopsy. *Ultrasound Obstet. Gynecol.*, 2000, **16**, 359–364.

284 Delle Chiaie, L. and **Terinde, R.** Three-dimensional ultrasound-validated large-core needle biopsy: is it a reliable method for the histological assessment of breast lesions? *Ultrasound Obstet. Gynecol.*, 2004, **23**, 393–397.

285 Kapur, A., Carson, P. L., Eberhand, J., Goodsitt, M. M., Thomenius, K., Lokhandwalla, M., Buckley, D., Roubidoux, M. A., Helvie, M. A., Booi, R. C., LeCarpentier, G. L., Erkamp, R. Q., Chan, H.-P., Fowlkes, J. B., Thomas, J. A., and **Landberg, C. E.** Combination of digital mammography with semi-automated 3D breast ultrasound. *Technol. Cancer Res. Treatment*, 2004, **3**(4), 325–334.

286 Matre, K., Stokke, E. M., Martens, D., and **Gilja, O. H.** *In vitro* volume estimation of kidneys using three-dimensional ultrasonography and a position sensor. *Eur. J. Ultrasound*, 1999, **10**, 65–73.

287 Gilja, O. H., Smievoll, A. I., Thune, N., Matre, K., Hausken, T., Ødegaard, S., and **Berstad, A.** *In vivo* comparison of 3D ultrasonography and magnetic resonance imaging in volume estimation of human kidneys. *Ultrasound Med. Biol.*, 1995, **21**(1), 25–32.

288 Partik, B. L., Stadler, A., Schamp, S., Koller, A., Voracek, M., Heinz, G., and **Helbich, T. H.** 3D versus 2D ultrasound: accuracy of volume measurement in human cadaver kidneys. *Investigative Radiol.*, 2002, **37**(9), 489–495.

289 Ohishi, H., Hirai, T., Yamada, R., Hirohashi, S., Uchida, H., Hashimoto, H., Jibiki, T., and **Takeuchi, Y.** Three-dimensional power Doppler sonography of tumor vascularity. *J. Ultrasound Med.*, 1998, **17**(10), 619–622.

290 Zubarev, A. V. Ultrasound of renal vessels. *Eur. Radiol.*, 2001, **11**(10), 1902–1915.

291 Mohaupt, M. G., Perrig, M., and **Vogt, B.** 3D ultrasound imaging – a useful non-invasive tool to detect AV fistulas in transplanted kidneys. *Nephrol. Dialysis Transplantation*, 1999, **14**, 940–943.

292 Leroy, A., Mozer, P., Payan, Y., and **Troccaz, J.** Rigid registration of freehand 3D ultrasound and CT-scan kidney images. In Proceedings of the Seventh International Conference on *Medical image computing and computer-assisted intervention (MICCAI 2004)*, Lecture Notes in Computer Science, Vol. 3216, Saint-Malo, France, 26–29 September 2004, Part I, pp. 837–844 (Springer-Verlag, Berlin).

293 Gilja, O. H., Trygve, H., Ødegaard, S., and **Berstad, A.** Ultrasonography and three-dimensional methods of the upper gastrointestinal tract. *Eur. J. Gastroenterol. Hepatol.*, 2005, **17**(3), 277–282.

294 Nishimura, K., Niwa, Y., Goto, H., Hase, S., Arisawa, T., and **Hayakawa, T.** Three-dimensional endoscopic ultrasonography of gastrointestinal lesions using an ultrasound probe. *Scand. J. Gastroenterol.*, 1997, **32**(9), 862–868.

295 Gilja, O. H., Hausken, T., Ødegaard, S., and **Berstad, A.** Three-dimensional ultrasonography of the gastric antrum in patients with functional dyspepsia. *Scand. J. Gastroenterol.*, 1996, **31**(9), 847–855.

296 Hünerbein, M., Ghadimi, B. M., Gretschel, S., and **Schlag, P. M.** Three-dimensional endoluminal ultrasound: a new method for the evaluation of gastrointestinal tumors. *Abdominal Imaging*, 1999, **24**, 445–448.

297 Liu, J. B., Miller, L. S., Bagley, D. H., and **Goldberg, B. B.** Endoluminal sonography of the genitourinary and gastrointestinal tracts. *J. Ultrasound Med.*, 2002, **21**, 323–337.

298 Mundt, M. W., Hausken, T., Smout, A. J. P. M., and **Samsom, M.** Relationships between gastric accommodation and gastrointestinal sensations in healthy volunteers: A study using the barostat technique and two- and three-dimensional ultrasonography. *Digestive Dis. Sci.*, 2005, **50**(9), 1654–1660.

299 Gilja, O. H., Detmer, P. R., Jong, J. M., Leotta, D. F., Li, X. N., Beach, K. W., Martin, R., and **Strandness Jr, D. E.** Intragastric distribution and gastric emptying assessed by three-dimensional ultrasonography. *Gastroenterology*, 1997, **113**, 38–49.

300 Scheffer, R. C. H., Gooszen, H. G., Wassenaar, E. B., and **Samsom, M.** Relationship between partial gastric volumes and dyspeptic symptoms in fundoplication patients: a 3D ultrasonographic

study. *Am. J. Gastroenterol.*, 2004, **99**(10), 1902–1909.

301 van Lelyveld, N., Scheffer, R., Mundt, M., and **Samsom, M.** Partial gastric volumes and upper abdominal sensations in functional dyspeptic and GERD patients: a 3D ultrasonographic study. *Am. J. Gastroenterol.*, 2006, **101**(8), 1845–1852.

302 Bonilla-Musoles, F., Machado, L. E., Bailao, L. A., Osborne, N. G., and **Raga, F.** Abdominal wall defects: two- versus three-dimensional ultrasonographic diagnosis. *J. Ultrasound Med.*, 2001, **20**(4), 379–389.

303 Dai, Q., Brasseur, J. G., Dimitriou, J., Chung, C., Thomas, A., Assari, W., and **Miller, L. S.** 2-D and 3-D endoluminal ultrasound localization of endoscopic plications with simultaneous manometry (location of plications and depth of sutures). *Gastrointestinal Endoscopy*, 2004, **59**(5), P244.

304 Fritscher-Ravens, A., Knoefel, W. T., Christina, K., Swain, C. P., Brandt, L., and **Patel, K.** Three-dimensional linear endoscopic ultrasound – feasibility of a novel technique applied for the detection of vessel involvement of pancreatic masses. *Am. J. Gastroenterol.*, 2005, **100**(6), 1296–1302.

305 Sjølie, E., Langø, T., Ystgaard, B., Tangen, G. A., Hernes, T. A. N., and **Mårvik, R.** 3D ultrasound-based navigation for radiofrequency thermal ablation in the treatment of liver malignancies. *Surg. Endoscopy*, 2003, **17**, 933–938.

306 Nakamoto, M., Sato, Y., Miyamoto, M., Nakamjima, Y., Konishi, K., Shimada, M., Hashizume, M., and **Tamura, S.** 3D ultrasound system using a magneto-optic hybrid tracker for augmented reality visualization in laparoscopic liver surgery. In Proceedings of the Fifth International Conference on *Medical image computing and computer-assisted intervention (MICCAI 2002)*, Lecture Notes in Computer Science, Vol. 2489, Tokyo, Japan, 25–28 September 2002, Part II, pp. 148–155 (Springer-Verlag, Berlin).

307 Sato, Y., Miyamoto, M., Nakamoto, M., Nakamjima, Y., Shimada, M., Hashizume, M., and **Tamura, S.** 3D ultrasound image acquisition using a magneto-optic hybrid sensor for laparoscopic surgery. In Proceedings of the Fourth International Conference on *Medical image computing and computer-assisted intervention (MICCAI 2001)*, Lecture Notes in Computer Science, Vol. 2208, Utrecht, The Netherlands, 14–17 October 2001, pp. 1151–1153 (Springer-Verlag, Berlin).

308 Harms, J., Feussner, H., Baumgartner, M., Schneider, A., Donhauser, M., and **Wessels, G.** Three-dimensional navigated laparoscopic ultrasonography first experiences with a new minimally invasive diagnostic device. *Surg. Endoscopy*, 2001, **15**, 1459–1462.

309 Boctor, E. M., Fichtinger, G., Taylor, R. H., and **Choti, M. A.** Tracked 3D ultrasound in radiofrequency liver ablation. In *Medical imaging 2003: ultrasonic imaging and signal processing*, Proceedings of the SPIE, Vol. 5035 (Eds W. F. Walker and M. F. Insana), 2003, pp. 174–182 (SPIE, Bellingham, Washington).

310 Lange, T., Eulenstein, S., Hünerbein, M., Lamecker, H., and **Schlag, P.-M.** Augmenting intraoperative 3D ultrasound with preoperative models for navigation in liver surgery. In Proceedings of the Seventh International Conference on *Medical image computing and computer-assisted intervention (MICCAI 2004)*, Lecture Notes in Computer Science, Vol. 3217, Saint-Malo, France, 26–29 September 2004, Part II, pp. 534–541 (Springer-Verlag, Berlin).

311 Ockenga, J., Gebel, M., Caselitz, M., Topalidis, T., Boozari, B., Bleck, J., and **Manns, M. P.** 3D-ultrasound in imaging, diagnosis and follow-up of an atypical hydatid cyst. *Z. Gastroenterol.*, 1998, **36**(7), 599–603.

312 Aylward, S. R., Jomier, J., and **Weeks, S.** Intraoperative 3D ultrasound augmentation. In Proceedings of the IEEE International Symposium on *Biomedical Imaging*, 2002, pp. 421–424 (IEEE, New York).

313 Lange, T., Eulenstein, S., Hünerbein, M., and **Schlag, P.-M.** Vessel-based non-rigid registration of MR/CT and 3D ultrasound for navigation in liver surgery. *Comput. Aided Surg.*, 2003, **8**(5), 228–240.

314 Lindseth, F., Langø, T., Bang, J., and **Hernes, T. A. N.** Accuracy evaluation of a 3D ultrasound-based neuronavigation system. *Comput. Aided Surg.*, 2002, **7**, 197–222.

315 Lunn, K. E., Hartov, A., Kennedy, F. E., Miga, M. I., Roberts, D. W., Platenik, L. A., and **Paulsen, K. D.** 3D ultrasound as sparse data for intraoperative brain deformation model. In *Medical imaging 2001: ultrasonic imaging and signal processing*, Proceedings of the SPIE, Vol. 4375 (Eds M. F. Insana and K. K. Shung), 2001, pp. 326–332 (SPIE, Bellingham, Washington).

316 Unsgaard, G., Selbekk, T., Müller, T. B., Ommedel, S., Torp, S. H., Myhr, G., Bang, J., and **Hernes, T. A. N.** Ability of navigated 3D ultrasound to delineate gliomas and metastases – comparison of image interpretations with histopathology. *Acta Neurochir.*, 2005, **147**, 1259–1269.

317 Lindseth, F., Ommedal, S., Bang, J., Unsgård, G., and **Nagelhus Hernes, T. A.** Image fusion of ultrasound and MRI as an aid for assessing anatomical shifts and improving overview and interpretation in ultrasound-guided neurosurgery. In *CARS 2001: computer assisted radiology and surgery*, International Congress Series, Vol. 1230, 2001, pp. 254–260 (Elsevier, Amsterdam).

318 Bonsanto, M. M., Staubert, A., Wirtz, C. R., Tronnier, V., and **Kunze, S.** Initial experience with an ultrasound-integrated single-rack neuronavigation system. *Acta Neurochir.*, 2001, **143**, 1127–1132.

319 Gronningsaeter, A., Lie, T., Kleven, A., Mørland, T., Langø, T., Unsgård, G., Myhre, H. O., and

Mårvik, R. Initial experience with stereoscopic visualization of three-dimensional ultrasound data in surgery. *Surg. Endoscopy*, 2000, **14**, 1074–1078.

320 Lindner, D., Trantakis, C., Arnold, S., Schmitgen, A., Schneider, J., and **Meixenberger, J.** Neuronavigation based on intraoperative 3D-ultrasound during tumor resection. In *CARS 2005: computer assisted radiology and surgery*, International Congress Series, Vol. 1281, 2005, pp. 815–820 (Elsevier, Amsterdam).

321 Letteboer, M. M. J., Willems, P. W. A., Viergever, M. A., and **Niessen, W. J.** Non-rigid registration of 3D ultrasound images of brain tumours acquired during neurosurgery. In Proceedings of the Sixth International Conference on *Medical image computing and computer-assisted intervention (MICCAI 2003)*, Lecture Notes in Computer Science, Vol. 2879, Montréal, Canada, 15–18 November 2003, pp. 408–415 (Springer-Verlag, Berlin).

322 Lindner, D., Trantakis, C., Renner, C., Arnold, S., Schmitgen, A., Schneider, J., and **Meixensberger, J.** Application of intraoperative 3D ultrasound during navigated tumor resection. *Minimally Invasive Neurosurg.*, 2006, **49**(4), 197–202.

323 Gobbi, D. G., Comeau, R. M., Lee, B. K. H., and **Peters, T. M.** Integration of intra-operative 3D ultrasound with pre-operative MRI for neurosurgical guidance. In Proceedings of the 22nd Annual Engineering in Medicine and Biology Society International Conference, Chicago, Illinois, USA, 23–28 July 2000, pp. 1738–1740 (IEEE, New York).

324 Gobbi, D. G. and **Peters, T. M.** Interactive intraoperative 3D ultrasound reconstruction and visualization. In Proceedings of the Fifth International Conference on *Medical image computing and computer-assisted intervention (MICCAI 2002)*, Lecture Notes in Computer Science, Vol. 2489, Tokyo, Japan, 25–28 September 2002, Part II, pp. 156–163 (Springer-Verlag, Berlin).

325 Unsgaard, G., Rygh, O. M., Selbekk, T., Müller, T. B., Kolstad, F., Lindseth, F., and **Nagelhus Hernes, T. A.** Intra-operative 3D ultrasound in neurosurgery. *Acta Neurochir.*, 2006, **148**, 235–253.

326 Comeau, R. M., Sadikot, A. F., Fenster, A., and **Peters, T. M.** Intraoperative ultrasound for guidance and tissue shift correction in image-guided neurosurgery. *Med. Phys.*, 2000, **27**(4), 787–800.

327 Woydt, M., Horowski, A., Krauss, J., Krone, A., Soerensen, N., and **Roosen, K.** Three-dimensional intraoperative ultrasound of vascular malformations and supratentorial tumors. *J. Neuroimaging*, 2002, **12**(1), 28–34.

328 Gobbi, D. G., Comeau, R. M., and **Peters, T. M.** Ultrasound/MRI overlay with image warping for neurosurgery. In Proceedings of the Third International Conference on *Medical image computing and computer-assisted intervention (MICCAI 2000)*, Lecture Notes in Computer Science, Vol. 1935, Pittsburgh, Pennsylvania, USA, 11–14 October 2000, pp. 106–114 (Springer-Verlag, Berlin).

329 Letteboer, M. M. J., Viergever, M. A., and **Niessen, W. J.** Rigid registration of 3D ultrasound data of brain tumours. In *CARS 2003: computer assisted radiology and surgery*, International Congress Series, Vol. 1256, 2003, pp. 433–439 (Elsevier, Amsterdam).

330 Fine, D., Perring, S., Herbetko, J., Hacking, C. N., Fleming, J. S., and **Dewbury, K. C.** Three-dimensional (3D) ultrasound imaging of the gall-bladder and dilated biliary tree: reconstruction of real-time b-scans. *Br. J. Radiol.*, 1991, **64**(767), 1056–1057.

331 Hausken, T., Søndenna, K., Svebak, S., Gilja, O. H., Olafsson, S., Ødegaard, S., Søreide, O., and **Berstad, A.** Common pathogenetic mechanisms in symptomatic, uncomplicated gallstone disease and functional dyspepsia volume measurement of gall-bladder and antrum using three-dimensional ultrasonography. *Digestive Dis. Sci.*, 1997, **42**(12), 2505–2512.

332 Mitkov, V. V. 3D ultrasound and diagnosis of gall-bladder diseases. *Ultrasound Med. Biol.*, 2006, **32**(5)(Suppl. 1), P76.

333 Himmelstine, L. G. 3D multiplanar images of the gall-bladder pathology. *Ultrasound Med. Biol.*, 2006, **32**(5)(Suppl. 1), P195–P196.

334 Acalovschi, M., Dumitrascu, D. L., Suteu, T., Veres, A., Albu, S., and **Badea, R. I.** Misoprostol induces gall-bladder contraction during fasting, but does not influence postprandial emptying: an ultrasound study in healthy subjects. *Acta Gastroenterol. Belg.*, 2002, **65**(4), 191–195.

335 Morimoto, A. K., Bow, W. J., Strong, D. S., Dickey, F. M., Krumm, J. C., Vick, D. D., Kozlowski, D. M., Partridge, S., Walsh, N., Faulkner, V., and **Rogers, B.** 3D ultrasound imaging for prosthesis fabrication and diagnostic imaging. Technical Report SAND94-3137. UC-906, Sandia National Laboratories, Albuquerque, New Mexico, USA, 1995.

336 Fuller, M. I., Blalock, T. N., Hossack, J. A., and **Walker, W. F.** A portable, low-cost, highly integrated, 3D medical ultrasound system. In Proceedings of the IEEE Ultrasonics Symposium, 2003, pp. 38–41 (IEEE, New York).

337 Sawada, A., Yoda, K., Kokubo, M., Kunieda, T., Nagata, Y., and **Hiraoka, M.** A technique for noninvasive respiratory gated radiation treatment system based on real time 3D ultrasound image correlation: a phantom study. *Med. Phys.*, 2004, **31**(2), 245–250.

338 Morsy, A. A. and **von Ramm, O. T.** 3D ultrasound tissue motion tracking using correlation search. *Ultrasonic Imaging*, 1998, **20**(3), 151–159.

339 Leven, J., Burschka, D., Kumar, R., Zhang, G., Blumenkranz, S., Dai, X., Awad, M., Hager, G. D., Marohn, M., Choti, M., Hasser, C., and **Taylor, R. H.** Davinci canvas: a telerobotic surgical system with integrated robot-assisted, laparoscopic ultra-

sound capability. In Proceedings of the Eighth International Conference on *Medical image computing and computer-assisted intervention (MICCAI 2005)*, Lecture Notes in Computer Science, Vol. 3749, Palm Springs, California, USA, 26–29 October 2005, Part I, pp. 811–818 (Springer-Verlag, Berlin).

340 **Huang, Q. H., Zheng, Y. P., Lu, M. H.,** and **Chi, Z. R.** Development of a portable 3D ultrasound imaging system for musculoskeletal tissues. *Ultrasonics*, 2005, **43**, 153–163.

341 **Baez, E., Huber, A., Vetter, M.,** and **Hackelöer, B.-J.** Minimal invasive complete excision of benign breast tumors using a three-dimensional ultrasound-guided mammotome vacuum device. *Ultrasound Obstet. Gynecol.*, 2003, **21**, 267–272.

342 **Pagoulatos, N., Rohling, R. N.,** and **Edwards, W. S.** New spatial localizer based on fiber optics with applications in 3D ultrasound imaging. In *Medical imaging 2000: image display and visualization*, Proceedings of the SPIE, Vol. 3976 (Ed. S. K. Mun), 2000, pp. 595–602 (SPIE, Bellingham, Washington).

343 **Stotzka, R., Widmann, H., Mueller, T. O., Schlote-Holubek, K., Gemmeke, H., Ruiter, N. V.,** and **Göbel, G.** Prototype of a new 3D ultrasound computer tomography system: transducer design and data recording. In *Medical imaging 2004: ultrasonic imaging and processing*, Proceedings of the SPIE, Vol. 5373 (Eds W. F. Walker and S. Y. Emelianov), 2004, pp. 70–79 (SPIE, Bellingham, Washington).

344 **Leung, K. Y., Ngai, C. S. W., Chan, B. C., Leung, W. C., Lee, C. P.,** and **Tang, M. H. Y.** Three-dimensional extended imaging: a new display modality for three-dimensional ultrasound examination. *Ultrasound Obstet. Gynecol.*, 2005, **26**, 244–251.

345 **Thiel, J. A., Suchet, I. B.,** and **Lortie, K.** Confirmation of Essure microinsert tubal coil placement with conventional and volume-contrast imaging three-dimensional ultrasound. *Fertility Sterility*, 2005, **84**(2), 504–508.

346 **Stoll, J., Navotny, P., Howe, R.,** and **Dupont, P.** Real-time 3D ultrasound-based servoing of a surgical instrument. In Proceedings of the IEEE International Conference on *Robotics and Automation.*, 2006, pp. 613–618 (IEEE, New York).

347 **Ding, M.** and **Fenster, A.** Projection-based needle segmentation in 3D ultrasound images. In Proceedings of the Sixth International Conference on *Medical image computing and computer-assisted intervention (MICCAI 2003)*, Lecture Notes in Computer Science, Vol. 2879, Montréal, Canada, 15–18 November 2003, pp. 319–327 (Springer-Verlag, Berlin).

348 **Peters, T. M.** Image-guidance for surgical procedures. *Phys. Med. Biol.*, 2006, **51**(14), R505–R540.

349 **Kuban, D. A., Dong, L., Cheung, R., Strom, E.,** and **De Crevoisier, R.** Ultrasound-based localization. *Semin. Radiation Oncol.*, 2005, **15**(3), 180–191.

350 **Sauer, G., Deissler, H., Strunz, K., Helms, G., Remmel, E., Koretz, K., Terinde, R.,** and **Kreienberg, R.** Ultrasound-guided large-core needle biopsies of breast lesions: analysis of 962 cases to determine the number of samples for reliable tumour classification. *Br. J. Cancer*, 2005, **92**(2), 231–235.

351 **Benacerraf, B., Bromley, B.,** and **Shipp, T.** Sonographic tomography – the application of 3D in every ultrasound unit. *Ultrasound Med. Biol.*, 2006, **32**(5)(Suppl. 1), P3–P4.

352 **Elliott, S. T.** Volume ultrasound: the next big thing? *Br. J. Radiol.*, 2008, **81**, 8–9.